The Astrophysical Journal, 703:675–691, 2009 September 20 doi:10.1088/0004-637X/703/1/675
© 2009. The American Astronomical Society. All rights reserved. Printed in the U.S.A.

KLEIN–NISHINA EFFECTS ON OPTICALLY THIN SYNCHROTRON AND SYNCHROTRON SELF-COMPTON SPECTRUM

Ehud Nakar[1,2], Shin'ichiro Ando[2], and Re'em Sari[2,3]
[1] Raymond and Beverly Sackler School of Physics & Astronomy, Tel Aviv University, Tel Aviv 69978, Israel
[2] California Institute of Technology, Mail Code 130-33, Pasadena, CA 91125, USA
[3] Racah Institute for Physics, The Hebrew University, Jerusalem 91904, Israel
Received 2009 January 1; accepted 2009 July 31; published 2009 August 31

ABSTRACT

We present analytic approximations to the optically thin synchrotron and synchrotron self-Compton (SSC) spectra when Klein–Nishina (KN) effects are important and pair production and external radiation fields can be neglected. This theory is useful for analytical treatment of radiation from astrophysical sources, such as gamma-ray bursts (GRBs), active galactic nuclei, and pulsar wind nebula, where KN effects may be important. We consider a source with continuous injection of relativistic electrons with a power-law energy distribution above some typical injection energy. We find that the synchrotron-SSC spectra can be described by a broken power law, and provide analytic estimates for the break frequencies and power-law indices. In general, we show that the dependence of the KN cross section on the energy of the upscattering electron results in a hardening of the energy distribution of fast cooling electrons and therefore in a hardening of the observed synchrotron spectrum. As a result the synchrotron spectrum of fast cooling electrons, below the typical injection energy, can be as hard as $F_\nu \propto \nu^0$, instead of the classical $\nu^{-1/2}$ when KN effects are neglected. The synchrotron energy output can be dominated by electrons with energy above the typical injection energy. We solve self-consistently for the cooling frequency and find that the transition between synchrotron and SSC cooling can result in discontinuous variations of the cooling frequency and the synchrotron and SSC spectra. We demonstrate the application of our results to theory by applying them to prompt and afterglow emission models of GRBs.

Key words: galaxies: active – gamma rays: bursts – pulsars: general – radiation mechanisms: non-thermal

Online-only material: color figures

1. INTRODUCTION

Synchrotron and synchrotron self-Compton (SSC) are common radiation processes in astrophysical environments where relativistic electrons are continuously injected into a magnetized plasma. In the Thomson scattering regime, the SSC component dominates the energy output whenever the local energy density of the synchrotron photons is larger than the energy density of the local magnetic field, as well as the energy density of any external radiation field. In such a case, synchrotron photons that are upscattered once by the synchrotron emitting electrons carry more energy than the unscattered synchrotron photons. The typical frequency of the upscattered photons is increased by a factor of $\sim \gamma^2$, where γ is the typical electron Lorentz factor. Photons that are upscattered twice carry more energy than those that are scattered once and there typical frequency is again multiplied by $\sim \gamma^2$. This hierarchical spectral structure, where the total photons energy increases with the number of scattering and the frequency of each generation is shifted by γ^2, continues up to the point where the energy of the upscattered photons gets to the Klein–Nishina (KN) limit. Namely, the individual photon energy, as measured in the rest frame of the upscattering electron, becomes comparable to the electron rest-mass energy, $m_e c^2$. At this point, there is a transition of the scattering cross section from the constant Thomson regime to the KN regime, where it is inversely proportional to the photons frequency. In addition, the photon energy gain at each scattering (frequency shift), which is proportional to the pre-scattering photon energy in the Thomson regime, becomes constant (roughly $\gamma m_e c^2$) above the KN limit. The cross section falloff and the saturation of the energy transfer at each scattering, terminate the hierarchical spectral structure above the KN limit.

The direct effect of the KN limit on the observed spectrum is the suppression of high-energy upscattered photons. However, an indirect effect is present in the case that SSC emission dominates the energy output, and that at least some of the injected electrons have enough time to cool. In such a case, electrons with different energies (Lorentz factors) are cooling on a different fraction of the radiation field. The reason is that some of the photons that are below the KN limit for less energetic electrons are above this limit for more energetic electrons. As a result, the energy distribution of the cooling electrons is modified by the KN limit, and so does the synchrotron spectrum as well as the spectra of all the SSC hierarchical branches. While this indirect effect is less dramatic than the high-energy KN cutoff, it may be the only observed KN effect in cases that the high-energy SSC branches are above the detectors energy range, thereby providing a valuable information about the physical properties of the source. Moreover, the KN modified synchrotron spectrum may be significantly different than the unmodified one, making it necessary to include KN effects even in cases where just the synchrotron spectrum is analyzed.

In relativistic sources, such as active galactic nuclei (AGNs) and gamma-ray bursts (GRBs), it is thought that optically thin synchrotron and SSC emission is produced behind relativistic shocks, where a fresh population of relativistic electrons is injected. Analytic approximation of the synchrotron-SSC spectra in such systems is rather complex even when the KN feedback on the electron distribution are not fully accounted for (e.g., Meszaros et al. 1994; Tavecchio et al. 1998; Petry et al. 2000; Dermer et al. 2000; Sari & Esin 2001; Böttcher & Dermer 2002; Fan & Piran 2006; Zhang et al. 2007). Rees (1967) derived the set of equations which self-consistently follow the electron distribution for a one-zone synchrotron-SSC model (when pair

production can be ignored) and solved them numerically for several examples in the context of radio sources. Numerical calculations for different sources (e.g., GeV, AGNs, and GRBs), and with additional physics (e.g., time-dependent photon field and pair production) followed (e.g., Coppi 1992; Mastichiadis & Kirk 1997; Li & Kusunose 2000; Pe'er & Waxman 2005b; Fan et al. 2008; Vurm & Poutanen 2009). However, useful analytic approximations of the optically thin synchrotron-SSC spectra in cases that KN effects are important, were only partially discussed for a few special cases (Derishev et al. 2003; Pe'er & Waxman 2005a; Ando et al. 2008).

The purpose of this paper is to provide an analytic approximation of the optically thin synchrotron and SSC spectra in cases where KN feedback plays an important role and cannot be ignored, while pairs production can be ignored. We consider a relativistic blast wave that injects electrons with a power-law energy distribution and provides a comprehensive analytic approximate description of the resulting spectra as a function of the importance of the KN suppression and the relative cooling by synchrotron and SSC. We provide an analytic formula for the SSC to synchrotron energy output ratio as a function of the physical parameters. These approximations are useful as guidelines of the expected range of possible optically thin synchrotron-SSC spectra and as a tool for interpretation of observation without carrying out elaborate numerical calculations. The limitation of the analytic approach is that it provides a sharp broken power-law spectrum, while the true spectra are quite smooth. Since KN effects on the electron spectrum are resulting from integration over the electron spectrum itself (see Equation (15)), the synchrotron power-law-breaks that are associated with KN effects are smoother than those that are not. Nevertheless, the approximated analytic spectra provided here are by far more accurate than calculations (numerical or analytic) that neglect KN effects on the electron spectrum. We caution that these calculations apply only when the source is optically thin and pair production can be neglected. This is not a trivial demand, since photons that are upscattered near the KN limit are energetic enough to produce pairs with the seed photons. Thus, pair production can be neglected only when the source is optically thin not only to Thomson scattering on electrons/pairs but also to pair creation by energetic photons on the seed photons. While the later condition is more stringent (since seed photons are more numerous than optically thin electrons/pairs), it is still applicable to many astrophysical sources.

Our results show that since lower-energy electrons are cooling more efficiently by SSC emission, KN effects result in harder spectra of electrons that are cooling fast (i.e., radiating most of their energy over the system lifetime). We show that in case that electrons are continuously injected with some minimal Lorentz factor γ_m and all the electrons are cooling fast, the spectrum of the synchrotron flux at frequencies that are below $\nu_{\rm syn}(\gamma_m)$ can be, in extreme cases, as hard as $F_\nu \propto \nu^0$ (compared to the typical $F_\nu \propto \nu^{-1/2}$, where $\nu_{\rm syn}$ is the synchrotron frequency). We also show that the spectrum at $\nu > \nu_m$ can be hard enough, so most of the synchrotron energy is emitted at $\nu > \nu_m$ even if most of the injected electron energy is in electrons with Lorentz factor of the order of γ_m which are cooling fast. Another KN effect is that the transition from electrons that are cooling fast by synchrotron emission to electrons that are cooling fast by SSC emission can result in a dramatic observational signature where the observed spectral break that corresponds to the cooling Lorentz factor (above which electrons are cooling fast) "jumps" by orders of magnitude within a short time.

KN effects increase the complexity of the observed spectra and the number of different types of spectra. In the paper, we separate the observed spectra to six different types, which cover the most relevant possibilities, each corresponding to different physical conditions in the source. For convenience, Table 1 summarizes the observed spectral types that correspond each to a given physical system and gives the references to the equations that are relevant to each case. Tables 2–4 list the values of the break frequencies and of the spectral power-law indices for each of the different cases. A reader that is interested only in the specific spectrum of a given physical system can start the search in Table 1.

The paper is organized as follows: in Section 2, we describe the physical model and present guidelines of the general considerations that we use to derive the synchrotron-SSC analytic spectra in the different cases. Spectra of systems where all the electrons are cooling fast are derived in Section 3 and spectra of systems where most of the energy is in electrons that cool slowly are presented in Section 4. The exact definition and value of the cooling frequency, as well as its effects on the observed spectrum, are discussed in Section 5. We demonstrate the application of our results to theory by applying them to prompt and afterglow emission models of GRBs in Section 6. The main results are summarized in Section 7.

2. SYNCHROTRON-SSC SPECTRA—GENERAL CONSIDERATIONS

We consider a one-zone model where relativistic electrons radiate synchrotron emission and where the inverse-Compton emission of these electrons is dominated by upscattering their own emitted synchrotron photons. The electron population in the source is generated by a continuous injection of relativistic electrons with a power-law distribution, i.e., $Q \propto \gamma^{-p}$ for $\gamma > \gamma_m$ ($Q = 0$ otherwise), where Q is the electron source function, γ is the electron Lorentz factor, and $p > 2$. We consider only radiative cooling and define γ_c as the Lorentz factor above which electrons are cooled efficiently over the age of the system.[4] The source is optically thin to photons emitted at the typical synchrotron frequency, so self-absorption can be ignored. The source is also optically thin for pair production by an arbitrarily energetic photon on the synchrotron photons, so pair production can be neglected. We also neglect short timescale variability of the photon field in the sense that we work in the regime where the photon field is determined by instantaneous electron distribution. Finally, cosmological redshift effects are neglected in this study. These can be easily added to the results according to the usual prescription.

The scenario of interest here is the one where the energy density of synchrotron photons in the source is larger than the magnetic field energy density, since only in this regime the electrons distribution depends on KN effects, as the cooling of some of the electrons is dominated by SSC while others are cooled predominantly by synchrotron radiation. Therefore throughout the paper we assume that the synchrotron energy density dominates over the magnetic field energy density, with the exception of Sections 3.5 and 4.1 where, for completeness, we briefly discuss the SSC spectra when synchrotron radiation dominates the cooling of all electrons. Finally, we discuss here in detail only the case where the KN limit is relevant for

[4] As a result of KN effects, the definition of γ_c may be more complicated in a small region of the parameter space. We discuss the definition (and value) of γ_c in Section 5.

Table 1
Physical Conditions and the Corresponding Observed Spectral Case

Case	Condition 1	Condition 2[a]	Condition 3	Section	Y[b]	$F_\nu^{\rm syn}$[b]	$F_\nu^{\rm IC}$[b]
Case I (Fast)	$\nu_m < \widehat{\nu_m}$	$\sqrt{\frac{\epsilon_e}{\epsilon_B}} < \frac{\gamma_m}{\gamma_c}$	$\gamma_c^{\rm syn} < \sqrt{\frac{\epsilon_e}{\epsilon_B}}\gamma_m$	$\left(\frac{\gamma_0}{\gamma_m}\right)^{2p-4} > \frac{\epsilon_e}{\epsilon_B}$	3.1	19	21	23
		$\sqrt{\frac{\epsilon_e}{\epsilon_B}} > \frac{\gamma_m}{\gamma_c}$			3.1	19	22	24
		$\sqrt{\frac{\epsilon_e}{\epsilon_B}} < \frac{\gamma_m}{\gamma_c}$		$\left(\frac{\gamma_0}{\gamma_m}\right)^{2p-4} < \frac{\epsilon_e}{\epsilon_B}$	3.1.1	19+25	21+25	...
Case IIa (Fast)	$\frac{\epsilon_e}{\epsilon_B} < \left(\frac{\gamma_m}{\widehat{\gamma_m}}\right)^{\frac{1}{3}}$	$\gamma_c^{\rm syn} < \gamma_m$		3.2.1	28	29	text
Case IIb (Fast)	$\left(\frac{\gamma_m}{\widehat{\gamma_m}}\right)^{\frac{1}{3}} < \frac{\epsilon_e}{\epsilon_B} < \frac{\gamma_m}{\widehat{\gamma_m}}$	$\gamma_c^{\rm syn} < \gamma_m$		3.2.1	31	32	text
Case IIc (Fast)	$\frac{\gamma_m}{\widehat{\gamma_m}} < \frac{\epsilon_e}{\epsilon_B} < \left(\frac{\gamma_m}{\widehat{\gamma_m}}\right)^3$	$\gamma_c^{\rm syn} < \gamma_{c,\max,0}$	$2 < p < 3$	3.2.3	34	35	text
			$p > 3$		text	text	...
Case III (Fast)	$\gamma_m = \widehat{\gamma_m}$	$\gamma_c^{\rm syn} < \gamma_{c,\max,0}$	$2 < p < 2.5$	3.3	37	38	39
			$p > 2.5$		text	text	text
Slow cooling		Not fast	$2 < p < 3$	4	46+47	48	50

Notes. A summary of the physical conditions that correspond to any of the spectral cases and subcases discussed in the paper. In order to find the relevant spectrum the conditions are applied from left to right in the following logic sequence: *"if cond 1, then if cond 2, then if cond 3, then..."*. If all conditions are satisfied then the relevant case is discussed in relevant section and the relevant equation numbers of Y, $F_\nu^{\rm syn}$ and $F_\nu^{\rm IC}$ are indicated.
[a] The condition for fast or slow cooling regime. $\gamma_c^{\rm syn} \equiv (6\pi m_e c)/(\sigma_T B^2 t)$ depends on the physical parameters of the system (it is the value of the synchrotron cooling frequency if SSC emission is ignored). The spectrum is in the slow cooling regime in case that *cond 1* of any of the fast cooling phases is satisfied but the corresponding *cond 2* is not satisfied (e.g., if $\nu_m < \widehat{\nu_m}$ but $\gamma_c^{\rm syn} > \gamma_m\sqrt{\epsilon_e/\epsilon_B}$).
[b] The number of the relevant equation. When the entree is *"text"* then this case is discussed in the text of the relevant section.

the synchrotron photons, implying that multiple scattering are strongly suppressed and only single scattering SSC is important. The case where there are multiple SSC generations is not discussed here but it shows similar effects and similar values of the asymptotic power-law indices to those of the single generation case.

The self-consistent electron distribution and the observed spectra can be easily computed once we know the synchrotron to SSC emissivity ratio as a function of the electron Lorentz factor

$$Y(\gamma) \equiv \frac{P_{\rm SSC}(\gamma)}{P_{\rm syn}(\gamma)}. \quad (1)$$

When KN effects are neglected, $Y \equiv Y_{\rm noKN}$ is constant and we first rederive its value (e.g., Sari & Esin 2001). The scenario that we have in mind is an emission from a plasma that is heated by a relativistic shock where relativistic electrons are injected at the shock front and carry a fraction ϵ_e out of the injected internal energy. The fraction of the magnetic field energy out of the internal energy in the shocked plasma is ϵ_B. In this case,

$$Y_{\rm noKN} \approx \frac{U_{\rm syn}}{U_B} \approx \frac{\eta\epsilon_e}{(1+Y_{\rm noKN})\epsilon_B}, \quad (2)$$

where $U_{\rm syn}$ and U_B are the energy density of synchrotron photons and magnetic field respectively and $\eta = \min\{1, (\gamma_m/\gamma_c)^{p-2}\}$ is the fraction of electrons energy that was emitted. Therefore

$$Y_{\rm noKN} \approx \begin{cases} \sqrt{\frac{\eta\epsilon_e}{\epsilon_B}} & Y_{\rm noKN} \gg 1 \\ \frac{\eta\epsilon_e}{\epsilon_B} & Y_{\rm noKN} \ll 1. \end{cases} \quad (3)$$

When relating $\frac{U_{\rm syn}}{U_B}$ to $\frac{\epsilon_e}{\epsilon_B}$ we assume that the volume occupied by the shocked plasma, $V_{\rm plasma}$, is comparable to the volumed occupied by synchrotron radiation, $V_{\rm rad}$. This is true for the relativistic shocks considered here but is not necessarily correct in the general case. In case that $V_{\rm plasma} \ll V_{\rm rad}$, then Equation (2) is generalized by multiplying the right-hand side by the fraction of the photon energy that is contained within $V_{\rm plasma}$. In the case of a non-relativistic blast wave with velocity $v_{\rm sh}$, this fraction is roughly $v_{\rm sh}/c$ (Sari & Esin 2001). This is the only generalization needed in order to apply the results of this paper to cases where $V_{\rm plasma} \ll V_{\rm rad}$.

The line of reasoning used to derive Equation (2) can be used to show that in general when electrons with Lorentz factor γ are fast cooling by upscattering their own synchrotron photons then $Y(\gamma)(1+Y(\gamma)) \approx \epsilon_e(\gamma)/\epsilon_B$, where $\epsilon_e(\gamma)$ is the fraction of energy injected in electrons with Lorentz factor γ.

In order to understand the effects of the KN limit it is useful to define the following function of an electron Lorentz factor

$$\widehat{\gamma} = \frac{m_e c^2 \Gamma}{h\nu_{\rm syn}(\gamma)} \propto \gamma^{-2}, \quad (4)$$

and its reciprocal function

$$\widetilde{\gamma} = \left(\frac{\gamma m_e c^2 \Gamma}{h\nu_{\rm syn}(\gamma)}\right)^{1/2} \propto \gamma^{-1/2}, \quad (5)$$

where m_e is the electron mass, c is the light speed, h is Planck's constant, Γ is the bulk Lorentz factor of the source (assuming the source is moving toward the observer), and $\nu_{\rm syn}(\gamma) \approx \Gamma\gamma^2 q_e B/(2\pi m_e c)$ is the typical observed frequency of the synchrotron emission of an electron with Lorentz factor γ (B is the magnetic field and q_e is the electron charge). These functions are useful since synchrotron photons emitted by electrons with Lorentz factor larger than γ (i.e., with frequency $> \nu_{\rm syn}(\gamma)$) cannot be upscattered efficiently by electrons with Lorentz factor larger than $\widehat{\gamma}$ because they are above the KN limit. Similarly, electrons with Lorentz factor γ cannot efficiently upscatter synchrotron photons emitted by electrons with Lorentz factor larger than $\widetilde{\gamma}$.

Table 2
Critical Lorentz Factor Values

Case		γ_0	$\widehat{\gamma_0}$	$\gamma_{c,\max,0}$	$\gamma_{c,\min,0}$
Case I (Fast)	$\sqrt{\frac{\epsilon_e}{\epsilon_B}} < \frac{\gamma_m}{\gamma_c}$	$\widehat{\gamma_m}\frac{\epsilon_e}{\epsilon_B}$	$^\dagger \frac{\gamma_m^2}{\widehat{\gamma_m}}\left(\frac{\epsilon_e}{\epsilon_B}\right)^{-2}$	...	...
	$\sqrt{\frac{\epsilon_e}{\epsilon_B}} > \frac{\gamma_m}{\gamma_c}$	$\widehat{\gamma_c}\left(\frac{\epsilon_e\gamma_c^2}{\epsilon_B\gamma_m^2}\right)^{\frac{3}{8}}$	$^\dagger \frac{\gamma_m^{3/2}\gamma_c^{1/2}}{\widehat{\gamma_c}}\left(\frac{\epsilon_e}{\epsilon_B}\right)^{-\frac{3}{4}}$	...	...
Case IIa (Fast)		$\widehat{\gamma_m}\left(\frac{\epsilon_e}{\epsilon_B}\right)^2$		...	...
Case IIb (Fast)	$\frac{\epsilon_e}{\epsilon_B} < \left(\frac{\gamma_m}{\widehat{\gamma_m}}\right)^{\frac{5}{6}}$	$\sqrt{\frac{\epsilon_e}{\epsilon_B}\gamma_m\widehat{\gamma_m}}$	$\gamma_m\left(\frac{\epsilon_e}{\epsilon_B}\right)^{-1}$	$\left(\frac{\epsilon_e}{\epsilon_B}\right)^{\frac{1}{3}}\gamma_m^{5/9}\widehat{\gamma_m}^{4/9}$	$\left(\frac{\epsilon_e}{\epsilon_B}\right)^{-\frac{4}{3}}\gamma_m^{\frac{10}{9}}\widehat{\gamma_m}^{-\frac{1}{9}}$
	$\frac{\epsilon_e}{\epsilon_B} > \left(\frac{\gamma_m}{\widehat{\gamma_m}}\right)^{\frac{5}{6}}$				$\left(\frac{\epsilon_e}{\epsilon_B}\right)^{-\frac{2}{3}}\gamma_m^{5/9}\widehat{\gamma_m}^{4/9}$
Case IIc (Fast)	$\frac{\epsilon_e}{\epsilon_B} < \left(\frac{\gamma_m}{\widehat{\gamma_m}}\right)^{\frac{4}{3}}$	$\sqrt{\frac{\epsilon_e}{\epsilon_B}\gamma_m\widehat{\gamma_m}}$	$\gamma_m\left(\frac{\epsilon_e}{\epsilon_B}\right)^{-1}$	$\left(\frac{\epsilon_e}{\epsilon_B}\right)^{\frac{1}{3}}\gamma_m^{5/9}\widehat{\gamma_m}^{4/9}$	$< \widehat{\gamma_m}$
	$\frac{\epsilon_e}{\epsilon_B} > \left(\frac{\gamma_m}{\widehat{\gamma_m}}\right)^{\frac{4}{3}}$			$\left(\frac{\epsilon_e}{\epsilon_B}\right)^{\frac{3}{7}}\gamma_m^{3/7}\widehat{\gamma_m}^{4/7}$	
Case III (Fast)	$p < 2.5$	$\gamma_m\left(\frac{\epsilon_e}{\epsilon_B}\right)^{\frac{3}{2(4-p)}}$	$\gamma_m\left(\frac{\epsilon_e}{\epsilon_B}\right)^{-\frac{3}{4-p}}$	$\gamma_m\left(\frac{\epsilon_e}{\epsilon_B}\right)^{3/7}$	$\left(\frac{\epsilon_e}{\epsilon_B}\right)^{-\frac{3}{14(2p-2)}}$
	$p > 2.5$	$\gamma_m\frac{\epsilon_e}{\epsilon_B}$		$\gamma_m\left(\frac{\epsilon_e}{\epsilon_B}\right)^{3/7}$	$\left(\frac{\epsilon_e}{\epsilon_B}\right)^{-1/14}$
Slow cooling	$2 < p < 3$	text	text	text	text

Notes. Critical values of γ that have an observable signature. These are given as a function of the ratio ϵ_e/ϵ_B and critical Lorentz factors γ_m, $\widehat{\gamma_m}$, γ_c and $\widehat{\gamma_c}$. The observed signature of γ_0 and $\widehat{\gamma_0}$ (when indicated) is a spectral break in ν_0 and $\widehat{\nu_0}$. The observed value of γ_c is always larger than $\gamma_{c,\max,0}$ or smaller than $\gamma_{c,\min,0}$ as intermediate value are not observed (see Section 5).

The KN limit introduces new critical Lorentz factors in addition to γ_m and γ_c,

$$\widehat{\gamma_m} = \frac{m_e c^2 \Gamma}{h\nu_m}, \qquad \widehat{\gamma_c} = \frac{m_e c^2 \Gamma}{h\nu_c}, \tag{6}$$

where $\nu_m \equiv \nu_{\rm syn}(\gamma_m)$ and $\nu_c \equiv \nu_{\rm syn}(\gamma_c)$,

$$\gamma_{\rm self} = \left(\frac{B_{\rm QED}}{B}\right)^{1/3} = \gamma^{2/3}\widehat{\gamma}^{1/3}, \tag{7}$$

which satisfies $\widehat{\gamma_{\rm self}} = \widetilde{\gamma_{\rm self}} = \gamma_{\rm self}$ and γ_0 which satisfies

$$Y(\gamma_0) = 1. \tag{8}$$

$B_{\rm QED} = 2\pi m_e^2 c^3/(q_e h) = 4.4 \times 10^{13}$ G is the quantum critical field. The requirement in this paper that the energy density of synchrotron photons in the source is larger than the magnetic field energy density guaranties that γ_0 is well defined. Note that this requirement is equivalent to $Y_{\rm noKN} > 1$ and therefore to $\eta\epsilon_e/\epsilon_B > 1$.

When KN effects are important, $Y(\gamma)$ is not a constant anymore and it affects the electron radiative cooling function

$$\frac{d\gamma}{dt} = -\frac{\sigma_T B^2}{6\pi m_e c}\gamma^2\left[1 + Y(\gamma)\right], \tag{9}$$

where t is the time as measured in the source rest frame ($t/2\Gamma$ is the time in the observer frame), σ_T is the Thomson cross section, and B is the magnetic field at time t. The continuity equation of the electron distribution reads

$$\frac{\partial N_\gamma}{\partial t} + \frac{\partial}{\partial\gamma}\left(N_\gamma\frac{d\gamma}{dt}\right) = Q, \tag{10}$$

where N_γ is the electron number per unit of γ. Here, we consider

$$Q = Q_0\begin{cases}0 & \gamma < \gamma_m\\ \left(\frac{\gamma}{\gamma_m}\right)^{-p} & \gamma > \gamma_m,\end{cases} \tag{11}$$

where Q_0 is constant and $p > 2$. Solving Equations (10) and (11), we find that the electron distribution can be approximated in the fast cooling regime (i.e., $\gamma_c < \gamma_m$) as

$$N_\gamma \propto \frac{1}{1+Y(\gamma)}\begin{cases}\gamma^{-2} & \gamma_c < \gamma < \gamma_m\\ \gamma^{-p-1} & \gamma_m < \gamma,\end{cases} \tag{12}$$

while in the slow cooling regime (i.e., $\gamma_m < \gamma_c$) it is

$$N_\gamma \propto \begin{cases}\gamma^{-p} & \gamma_m < \gamma < \gamma_c\\ \frac{1}{1+Y(\gamma)}\gamma^{-p-1} & \gamma_c < \gamma,\end{cases} \tag{13}$$

where in both regimes there are no electrons with $\gamma < \min\{\gamma_c, \gamma_m\}$. Equations (12) and (13) imply that the electron distribution depends significantly on $Y(\gamma)$ only if both $\gamma_c < \gamma$ and $Y(\gamma) > 1$ are satisfied (i.e., $\gamma_c < \gamma < \gamma_0$).

In general, the Y parameter can be approximated, in case of an isotropic photon field and ultra-relativistic electrons, as

$$Y(\gamma) = \frac{1}{U_B}\int_0^\infty \frac{dU_{\rm ph}}{d\nu}\int_{-1}^1 \frac{\frac{1}{2\sigma_T}(1-\mu)\sigma_{\rm KN}\left[\frac{\nu}{\widetilde{\nu}}(1-\mu)\right]}{1+\frac{\nu}{\widetilde{\nu}}}d\mu d\nu, \tag{14}$$

where μ is the cosine of the angle between the upscattered photon and the scattering electron momenta in the source frame and $\sigma_{\rm KN}[x]$ is the KN cross section for scattering of photons with energy $h\nu = xm_e c^2$ in the electron's rest frame. The numerator in the integral over μ gives the rate at which photons with a frequency ν and incident angle μ are upscattered, normalized to the rate in the Thomson scattering regime. The factor $1/(1+\nu/\widetilde{\nu})$ is approximately the energy given

Table 3
Synchrotron Power-law Indices that Result from KN Effects

Index[a]	Case—Frequency Range[b]	Origin[c]
0	IIb - $\widehat{\nu_0} < \nu < \nu_0$	$\gamma_c < \gamma < \gamma_m$ electrons cool on photons from their own PLS
	IIc - $\widehat{\nu_m} < \nu < \nu_m$	
$-\frac{1}{4}$	IIa - $\widehat{\nu_m} < \nu < \nu_0$	$\gamma_c < \gamma < \gamma_m$ electrons cool on $F_\nu \propto \nu^{1/2}$ photons
	IIb - $\widehat{\nu_m} < \nu < \widehat{\nu_0}$	
$-\frac{p-1}{4}$	IIc - $\widehat{\nu_0} < \nu < \widehat{\nu_m}$	$\gamma_c < \gamma < \gamma_m$ electrons cool on $F_\nu \propto \nu^{(p-1)/2}$ photons
$-\frac{p-1}{3}$	III ($p < 2.5$) - $\widehat{\nu_0} < \nu < \nu_m$	$\gamma_c < \gamma < \gamma_m$ electrons cool on $F_\nu \propto \nu^{2(p-1)/3}$ photons
$-\frac{p}{2}+\frac{2}{3}$	I - $\widehat{\nu_c} < \nu < \nu_0$	$\max\{\gamma_c, \gamma_m\} < \gamma$ electrons cool on $\nu < \min\{\nu_c, \nu_m\}$ photons
	Slow - $\widehat{\nu_m} < \nu < \nu_0$	
$-\frac{p}{2}+\frac{1}{2}$	IIc - $\nu_m < \nu < \nu_0$	$\max\{\gamma_c, \gamma_m\} < \gamma$ electrons cool on $F_\nu \propto \nu^0$ photons
$-\frac{2(p-1)}{3}$	III - $\nu_m < \nu < \nu_0$	$\max\{\gamma_c, \gamma_m\} < \gamma$ electrons cool on $F_\nu \propto \nu^{(p-1)/3}$ photons
$-\frac{p}{2}+\frac{1}{4}$	I - $\widehat{\nu_m} < \nu < \widehat{\nu_c}$	$\max\{\gamma_c, \gamma_m\} < \gamma$ electrons cool on $F_\nu \propto \nu^{1/2}$ photons
$-\frac{3(p-1)}{4}$	Slow cooling -	$\max\{\gamma_c, \gamma_m\} < \gamma$ electrons cool on $F_\nu \propto \nu^{(p-1)/2}$ photons
	$\max\{\widehat{\nu_c}, \nu_c\} < \nu < \min\{\widehat{\nu_m}, \nu_0\}$	

Notes. The power-law segments (PLSs) that are introduced to the synchrotron spectrum by the KN limit.
[a] The power-law index of F_ν.
[b] The case and frequency range in which this PLS is observed.
[c] The physical origin of the corresponding PLS, i.e., the range of electron Lorentz factor values that dominate the synchrotron emission and the PLS of the synchrotron photons that dominates the cooling of these electrons.

Table 4
SSC Power-law Indices at $\nu > \nu^{\rm IC}_{\rm peak}$

Index	Origin (All Upscattering Electrons Have $\max\{\gamma_c, \gamma_m\} < \gamma$)
$-p+1$	$\widehat{\gamma_m} < \gamma < \gamma_0$ (fast cool)
	$\widehat{\gamma_c} < \gamma < \gamma_0$ (slow cool)
$-p+\frac{1}{2}$	Upscattering photons with $F^{\rm syn}_\nu \propto \nu^{-1/2}$
$-p+\frac{1}{4}$	Upscattering photons with $F^{\rm syn}_\nu \propto \nu^{-1/4}$
$-p$	Upscattering photons with $F^{\rm syn}_\nu \propto \nu^0$
$-p-\frac{1}{3}$	Upscattering photons with $F^{\rm syn}_\nu \propto \nu^{1/3}$

Notes. The SSC power-law indices of $F^{\rm IC}_\nu$ at $\nu > \nu^{\rm IC}_{\rm peak}$, which are a result of the KN limit. In all cases the electrons that dominate the emission in this range have lorentz factors $\gamma > \max\{\gamma_c, \gamma_m\}$. The power-law segment in the first row, $F^{\rm IC}_\nu \propto \nu^{-p+1}$, is observed whenever the upscattering electrons are within the Lorentz factor range indicated in the second columns. The other four power-law segments are observed whenever the SSC luminosity of electrons is dominated by upscattering photons from the synchrotron power-law indicated in the second column. See text for more details.

to each upscattered photon, again normalized to the energy given in the Thomson regime, where in the Thomson regime ($\nu/\widetilde{\nu} \ll 1$) photons gain energy that is proportional to their initial frequency, while in the KN regime ($\nu/\widetilde{\nu} > 1$) photons gain roughly a constant amount of energy ($\gamma m_e c^2$). Therefore, in the Thomson regime the integral over μ gives 1 while at the KN regime it is $\propto 1/\nu^2$ (neglecting logarithmic terms; note that $\sigma_{\rm KN}[x \gg 1] \propto \ln(2x)/x$). Therefore, if $d\ln(U_{\rm ph})/d\ln(\nu) < 2$ for all $\nu > \widetilde{\nu}$ then the integral over μ can be approximated as a Heaviside step function $H(\widetilde{\nu} - \nu)$ and Equation (14) reads $Y(\gamma) \approx U_{\rm ph}[\nu < \widetilde{\nu}]/U_B$.

If in addition to the step function approximation we further assume that there is no short timescale variability of the photon field (namely that the instantaneous emissivity determines the photon density) and that the volume occupied by the shocked plasma is equal to the volume occupied by the synchrotron radiation, we can write

$$Y(\gamma) = \frac{U_{\rm ph}[\nu < \widetilde{\nu}]}{U_B} = \frac{\epsilon_e}{\epsilon_B} \frac{(p-2)\int_0^{\widetilde{\nu}'(\gamma)} \int P'_{\nu',\rm syn}(\gamma^*) N_{\gamma^*} d\gamma^* d\nu'}{Q_0 m_e c^2 \gamma_m^2}, \quad (15)$$

where $P'_{\nu',\rm syn}(\gamma^*)$ is the synchrotron emissivity per frequency unit of an electron with Lorentz factor γ^* and $\widetilde{\nu}'(\gamma)$ is the synchrotron frequency of $\widetilde{\gamma}$ electron (note that both $\widetilde{\nu}'$ and $\widetilde{\gamma}$ are functions of γ), both measured in the plasma rest frame ($\widetilde{\nu}$ is the corresponding frequency as measured in the observer frame). The term $Q_0 m_e c^2 \gamma_m^2/(p-2)$ is the total electron energy injected into the emitting region per unit of time. Since we are looking for approximated power-law spectra the integrals of this equation can be approximated so:

$$Y(\gamma) \propto \begin{cases} \text{const} & \widetilde{\nu} > \nu^{\rm syn}_{\rm peak} \\ \gamma^{-\alpha(\widetilde{\gamma})-1} & \widetilde{\nu} < \nu^{\rm syn}_{\rm peak}, \end{cases} \quad (16)$$

where

$$\alpha(\widetilde{\gamma}) = \left.\frac{d\ln(F_\nu)}{d\ln(\nu)}\right|_{\widetilde{\nu}}, \quad (17)$$

F_ν is the observed energy flux per unit frequency and $\nu^{\rm syn}_{\rm peak}$ is the observed frequency which dominates the synchrotron energy output. Equation (16) can be understood as follows. As long as $\widetilde{\nu} > \nu^{\rm syn}_{\rm peak}$, the value of $U_{\rm ph}[\nu < \widetilde{\nu}]$ is dominated by $\nu^{\rm syn}_{\rm peak}$ photons and is therefore roughly constant. These electrons can inverse-Compton the photons containing most of the energy without suffering from the KN reduction. For $\widetilde{\nu} < \nu^{\rm syn}_{\rm peak}$, the SSC emissivity of γ electrons is dominated by upscattering $\widetilde{\nu}$ photons, implying $Y(\gamma) \propto \nu F_\nu|_{\widetilde{\nu}}$ and since $\widetilde{\nu} \propto \gamma^{-1}$ we obtain $Y(\gamma) \propto \gamma^{-\alpha(\widetilde{\gamma})-1}$. As discussed above, the approximation of the KN limit as a step function is valid as long as[5] $\alpha(\widetilde{\gamma}) < 1$. For $\alpha(\widetilde{\gamma}) > 1$, the increase in the photon energy density at frequencies larger than $\widetilde{\nu}$ overcompensate for the KN reduction, so the emissivity of γ electron is actually dominated by upscattering of photons with $\nu > \widetilde{\nu}$ deep in the KN regime and $Y(\gamma) \propto \gamma^{-2}$. Since in the spectral regimes considered in this paper $\alpha(\widetilde{\gamma}) < 1$ is always satisfied we use Equations (15) and (16) throughout the paper. Self-absorption results in spectra

[5] We use the step function approximation also when we numerically integrate over Equation (15) in order to evaluate the spectrum. We tested several cases to confirm that taking the accurate KN cross section and the average over all photons incident angles does not significantly affect the conclusions we draw based on numerical results. Its only effect in the cases discussed in this paper is to produce smoother light curves.

of $\alpha = 11/8$, $\alpha = 2$, or $\alpha = 5/2$ (see, e.g., Granot et al. 2000), and therefore all result in $Y(\gamma) \propto \gamma^{-2}$. We do not discuss self-absorption any further in this paper. Finally in order to close the set of equations we need to relate the power-law index of the synchrotron spectrum at $\nu_{\rm syn}(\gamma)$ to the electron distribution N_γ,

$$\alpha(\gamma) = \frac{1}{2}\left(\frac{{\rm d}\ln(N_\gamma)}{{\rm d}\ln(\gamma)} + 1\right). \quad (18)$$

A self-consistent solution of Equations (12) (or (13)), (16), and (18) can provide an analytic approximation of the observed spectrum. Examining those equations we can define several simple rules that will enable us to find the critical Lorentz factors in each case, and the corresponding frequencies where there are breaks in the synchrotron spectrum. First, in addition to the usual breaks at (the frequencies corresponding to) γ_m and γ_c there will be a break at γ_0, if $\gamma_0 > \gamma_c$. Next, a break in the synchrotron spectrum at some γ_b has a corresponding break in $Y(\gamma)$, if $\nu_{\rm syn}(\gamma_b) \leqslant \nu^{\rm syn}_{\rm peak}$ (Equation (16)). Now, a break in $Y(\gamma_b)$ results in a break in the electron distribution at $\widehat{\gamma_b}$ in case that $\gamma_c < \widehat{\gamma_b} < \gamma_0$ (Equations (12) and (13)). Thus, a break at some γ_b has a corresponding critical frequency at $\widehat{\gamma_b}$, given $\gamma_c < \widehat{\gamma_b} < \gamma_0$ and $\nu_{\rm syn}(\gamma_b) \leqslant \nu^{\rm syn}_{\rm peak}$. In principle, there can be a series of critical frequencies at $\gamma_b, \widehat{\gamma_b}, \widehat{\widehat{\gamma_b}}, \ldots$. The fact that $\widehat{\gamma} \propto \gamma^{-2}$ ensures that the series is terminated at some point with a frequency that is larger than γ_0 or smaller than γ_c. Furthermore, critical frequencies of second order or higher (i.e., $\widehat{\widehat{\gamma_b}}$, $\widehat{\widehat{\widehat{\gamma_b}}}$, etc.) can usually be neglected since they correspond to very mild breaks. Based on this algorithm to find the critical frequencies we can see that there are different types of spectra that are determined by the relations between γ_m, γ_c, γ_0, $\widehat{\gamma_m}$, $\widehat{\gamma_c}$, and $\widehat{\gamma_0}$. As it turns out, it is enough to know γ_m, γ_c, $\frac{\epsilon_e}{\epsilon_B}$, and one additional KN frequency, e.g, $\gamma_{\rm self}$, $\widehat{\gamma_m}$ or $\widehat{\gamma_c}$, to determine the relation between all different frequencies and to describe the entire spectral shape. While physically it is more natural to use $\gamma_{\rm self}$, we use $\widehat{\gamma_m}$ and/or $\widehat{\gamma_c}$ since there are observable spectral features corresponding to these Lorentz factors.

Below, we go over all possible relations between the critical frequencies and find six general types of synchrotron spectra. We shall discuss separately slow ($\gamma_m < \gamma_c$) and fast ($\gamma_c < \gamma_m$) cooling regimes, where the fast cooling regime is separated to cases where $\gamma_m < \widehat{\gamma_m}$, $\gamma_m = \widehat{\gamma_m}$, and $\gamma_m > \widehat{\gamma_m}$. The latter is the most complicated case and we divide it further into three subcases. For each case, we first present the value of $Y(\gamma)$, then the synchrotron spectrum and finally the SSC spectra. The value of γ_c and its evolution for each of the cases are discussed separately in Section 5. For convenience, we use the notation ν_x to denote the synchrotron frequency that corresponds to an electron with Lorentz factor γ_x. For example, $\nu_0 \equiv \nu_{\rm syn}(\gamma_0)$, $\widehat{\nu_m} \equiv \nu_{\rm syn}(\widehat{\gamma_m})$, $\widehat{\nu_c} \equiv \nu_{\rm syn}(\widehat{\gamma_c})$ etc.

3. FAST COOLING SPECTRA ($\gamma_c < \gamma_m$)

3.1. Case I—Weak KN Regime: $\gamma_m < \widehat{\gamma_m}$

Here, γ_0 and $\widehat{\gamma_c}$ are always larger than $\widehat{\gamma_m}$ but the order between them may vary, $\widehat{\widehat{\gamma_c}} < \gamma_c$ and is therefore unimportant. Typically, $\nu^{\rm syn}_{\rm peak} = \nu_m$ (unless $p \approx 2$ and $\widehat{\gamma_m}/\gamma_m$ is not too large; we discuss this special case in the Appendix) in which case $\widehat{\gamma_0}$ and $\widehat{\widehat{\gamma_m}}$ are larger than $\nu^{\rm syn}_{\rm peak}$ and are therefore irrelevant. γ_m electrons are cooling primarily on ν_m photons implying $Y(\gamma_m) \approx (\epsilon_e/\epsilon_B)^{1/2}$. When $\nu^{\rm syn}_{\rm peak} = \nu_m$, then all electrons with $\gamma < \widehat{\gamma_m}$ are also cooling on ν_m photons implying a constant $Y(\gamma < \widehat{\gamma_m})$. There are breaks in Y at $\widehat{\gamma_m}$ and $\widehat{\gamma_c}$ that correspond to spectral slopes $\alpha(\gamma_c < \gamma < \gamma_m) = -1/2$ and $\alpha(\gamma < \gamma_c) = 1/3$ respectively

$$Y(\gamma) = \begin{cases} \sqrt{\frac{\epsilon_e}{\epsilon_B}} & \gamma < \widehat{\gamma_m} \\ \sqrt{\frac{\epsilon_e}{\epsilon_B}}\left(\frac{\gamma}{\widehat{\gamma_m}}\right)^{-1/2} & \widehat{\gamma_m} < \gamma < \widehat{\gamma_c} \\ \sqrt{\frac{\epsilon_e}{\epsilon_B}}\frac{\gamma_c}{\gamma_m}\left(\frac{\gamma}{\widehat{\gamma_c}}\right)^{-4/3} & \widehat{\gamma_c} < \gamma. \end{cases} \quad (19)$$

According to this Y distribution

$$\gamma_0 = \begin{cases} \widehat{\gamma_m}\frac{\epsilon_e}{\epsilon_B} & \sqrt{\frac{\epsilon_e}{\epsilon_B}} < \frac{\gamma_m}{\gamma_c}; (\gamma_0 < \widehat{\gamma_c}) \\ \widehat{\gamma_c}\left(\frac{\gamma_c}{\gamma_m}\right)^{3/4}\left(\frac{\epsilon_e}{\epsilon_B}\right)^{3/8} & \sqrt{\frac{\epsilon_e}{\epsilon_B}} > \frac{\gamma_m}{\gamma_c}; (\gamma_0 > \widehat{\gamma_c}). \end{cases} \quad (20)$$

The corresponding synchrotron spectrum always has spectral breaks at ν_c, ν_m, $\widehat{\nu}$, and ν_0. In the case that $\gamma_0 < \widehat{\gamma_c}$ (i.e., $(\epsilon_e/\epsilon_B)^{1/2} < \gamma_m/\gamma_c$) these are the only break frequencies and the synchrotron spectrum is

$$F^{\rm syn}_\nu \propto \begin{cases} \nu^{-1/2} & \nu_c < \nu < \nu_m \\ \nu^{-p/2} & \nu_m < \nu < \widehat{\nu_m} \\ \nu^{-(p/2-1/4)} & \widehat{\nu_m} < \nu < \nu_0 \\ \nu^{-p/2} & \nu_0 < \nu. \end{cases} \quad (21)$$

An example of the analytic synchrotron spectrum, based on Equation (21) (with $\gamma_0 < \widehat{\gamma_c}$), and a comparison to numerically calculated spectrum is presented in Figure 1.

An additional break at $\widehat{\nu_c}$ is observed in case that $\widehat{\gamma_c} < \gamma_0$ (i.e., $(\epsilon_e/\epsilon_B)^{1/2} < \gamma_m/\gamma_c$),

$$F^{\rm syn}_\nu \propto \begin{cases} \nu^{-1/2} & \nu_c < \nu < \nu_m \\ \nu^{-p/2} & \nu_m < \nu < \widehat{\nu_m} \\ \nu^{-(p/2-1/4)} & \widehat{\nu_m} < \nu < \widehat{\nu_c} \\ \nu^{-(p/2-2/3)} & \widehat{\nu_c} < \nu < \nu_0 \\ \nu^{-p/2} & \nu_0 < \nu. \end{cases} \quad (22)$$

SSC spectrum. As $\gamma_c, \gamma_m \ll \widehat{\gamma_m}$ the SSC luminosity in this case is not significantly affected by KN cross section. Most of the energy is emitted around $2\nu_m\gamma_m^2$ and the spectrum is similar to the one described in Sari & Esin (2001) up to $\nu_{\rm IC}(\widehat{\gamma_m}) = 2\widehat{\gamma_m}^2\nu_m$. Electrons with $\widehat{\gamma_m} < \gamma < \gamma_0$ are still radiating practically all their energy to SSC and therefore the SSC spectrum is affected only mildly at $\nu \sim 2\widehat{\gamma_m}^2\nu_m$. The mild SSC break at this frequency arises from the fact that electrons with $\gamma < \widehat{\gamma_m}$ lose their energy to upscattering of ν_m photons, so $\nu_{\rm IC}(\gamma < \widehat{\gamma_m}) \propto \gamma^2$, while electrons with $\gamma > \widehat{\gamma_m}$ lose their energy by upscattering $\nu_m\frac{\widehat{\gamma_m}}{\gamma}$ photons, so $\nu_{\rm IC}(\gamma > \widehat{\gamma_m}) \propto \gamma$. As a result the SSC spectral index at $\nu > 2\widehat{\gamma_m}^2\nu_m$ is $p-1$ compared to $p/2$ at lower frequencies. If $\gamma_0 < \widehat{\gamma_c}$, then there is first a break at $\nu_{\rm IC}(\gamma_0)$ to a spectral index of $p - \frac{1}{2}$ and later at $\nu_{\rm IC}(\widehat{\gamma_c})$ to a spectral index of $p + \frac{1}{3}$. Therefore the SSC spectrum for $\gamma_0 < \widehat{\gamma_c}$ is

$$F^{\rm IC}_\nu \propto \begin{cases} \nu^{-p/2} & 2\nu_m\gamma_m^2 < \nu < 2\nu_m\widehat{\gamma_m}^2 \\ \nu^{-(p-1)} & 2\nu_m\widehat{\gamma_m}^2 < \nu < 2\nu_m\widehat{\gamma_m}\gamma_0 \\ \nu^{-(p-\frac{1}{2})} & 2\nu_m\widehat{\gamma_m}\gamma_0 < \nu < 2\nu_c\widehat{\gamma_c}^2 \\ \nu^{-(p+\frac{1}{3})} & 2\nu_c\widehat{\gamma_c}^2 < \nu. \end{cases} \quad (23)$$

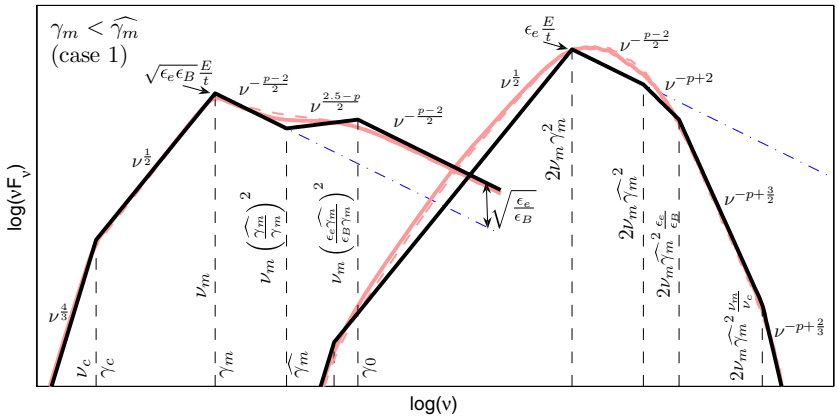

Figure 1. Synchrotron-SSC spectrum for $\gamma_c < \gamma_m < \widehat{\gamma_m}$ (Case I) and $\gamma_0 < \widehat{\gamma_c}$. The specific parameters are $\gamma_m/\widehat{\gamma_m} = 10^{-3}$, $\epsilon_e/\epsilon_B = 10^3$, and $p = 2.4$. The analytic spectrum (black line; see text) is compared to the numerical spectra, calculated by numerically integrating Equations (9), (10), and (15) (solid red line) and by integrating over 9, 10, and 14 (dashed red line). It is evident that the numerical spectra are smooth, where taking the actual KN cross section into account (Equation (14)) results in an additional smoothing over the step function approximation (Equation (15)). The value of the critical synchrotron frequencies is written next to the value of the corresponding electron Lorentz factor. The dash-dot lines are the spectrum in case that KN effects are ignored. Also noted are the synchrotron luminosity ($\sqrt{\epsilon_e/\epsilon_B}E/t$), SSC luminosity ($\epsilon_e E/t$) and the ratio of the synchrotron spectrum at $\nu_0 \ll \nu$ with and without including the KN limit ($\sqrt{\epsilon_e/\epsilon_B}$).
(A color version of this figure is available in the online journal.)

If $\widehat{\gamma_c} < \gamma_0$, then there is no break at $\nu_{\rm IC}(\widehat{\gamma_c})$ as the faster increase in the number of electrons above $\widehat{\gamma_c}$ compensates for the rapid decrease in the flux below γ_c. There is a break at $\nu_{\rm IC}(\gamma_0)$ directly to an index of $p + \frac{1}{3}$ and the SSC spectrum for $\gamma_c < \gamma_0$ is

$$F_\nu^{\rm IC} \propto \begin{cases} \nu^{-p/2} & \nu_m\gamma_m^2 < \nu < \nu_m\widehat{\gamma_m}^2 \\ \nu^{-(p-1)} & \nu_m\widehat{\gamma_m}^2 < \nu < \nu_m\widehat{\gamma_m}\gamma_0 \\ \nu^{-(p+\frac{1}{3})} & \nu_m\widehat{\gamma_m}\gamma_0 < \nu. \end{cases} \quad (24)$$

An example of the analytic SSC spectrum when $\gamma_0 < \widehat{\gamma_c}$ (Equation (23)), and its comparison to numerically calculated spectrum is presented in Figure 1. The normalization of the analytic spectrum is calculated using Equation (42).

3.1.1. Case I with $p \approx 2$

The discussion above is valid as long as $\nu_{\rm peak}^{\rm syn} = \nu_m$, which is the more common case. Nevertheless, if $(\gamma_m/\gamma_0)^{p-2}\sqrt{\epsilon_e/\epsilon_B} > 1$ the synchrotron energy output peaks at ν_0 and additional power-law segments are introduced. The exact spectrum depends on the ratio of energy injected in electrons with Lorentz factor of order γ_m to the energy injected in electrons with Lorentz factor of order γ_0. Here, we present the spectrum in case that this ratio is ≈ 1 (namely $(\gamma_m/\gamma_0)^{p-2} \approx 1$). In such a case, $\widehat{\widehat{\gamma_m}}$ and $\widehat{\gamma_0}$ (both smaller than γ_m) become critical frequencies (assuming that they are larger than γ_c). Electrons with $\gamma < \widehat{\widehat{\gamma_m}}$ experience enhanced SSC cooling, thereby suppressing the synchrotron emission at these frequencies. The energy flux at ν_0 is higher by a factor $\approx (\epsilon_e/\epsilon_B)^{1/2}$ than the one at ν_m, and therefore the flux at $\nu < \widehat{\nu_0}$ is suppressed by the same factor. As a result, additional power-law segments are introduced to Case I spectra (we assume here $\gamma_0 < \widehat{\gamma_c}$)

$$Y(\gamma) = \begin{cases} \frac{\epsilon_e}{\epsilon_B} & \gamma < \frac{\gamma_m^2}{\widehat{\gamma_m}}\left(\frac{\epsilon_e}{\epsilon_B}\right)^{-2} \\ \sqrt{\frac{\epsilon_e}{\epsilon_B}}\left(\frac{\gamma_m^2}{\widehat{\gamma_m}}\right)^{1/4}\gamma^{-1/4} & \frac{\gamma_m^2}{\widehat{\gamma_m}}\left(\frac{\epsilon_e}{\epsilon_B}\right)^{-2} < \gamma < \frac{\gamma_m^2}{\widehat{\gamma_m}}; \; p \approx 2. \\ F_\nu^{\rm syn} \propto \nu^{-3/8} & \max\{\nu_c, \widehat{\nu_0}\} < \nu < \widehat{\widehat{\nu_m}} \end{cases} \quad (25)$$

If $\widehat{\gamma_c} < \gamma_0$, then anther power-law segment is introduced to Y, but it does not affect the synchrotron spectrum.

Additional important property of this case is that the SSC to synchrotron luminosity ratio is significantly reduced (and is approximately unity), since electrons that are cooling primarily by synchrotron emit comparable amount of energy to those that are cooling by SSC (see discussion in Section 3.4).

3.2. Case II—Strong KN Regime: $\widehat{\gamma_m} < \gamma_m$

In this regime, $\widehat{\gamma_m} < \gamma_{\rm self} < \gamma_m$ and $\widehat{\gamma_m} < \gamma_0$. The shape of the spectrum depends mostly on the relations between γ_0, $\gamma_{\rm self}$, and γ_m. Therefore we divide this case to three subcases: (IIa) $\gamma_0 < \gamma_{\rm self} < \gamma_m$, (IIb) $\gamma_{\rm self} < \gamma_0 < \gamma_m$, and (IIc) $\gamma_{\rm self} < \gamma_m < \gamma_0$. The relevant case for a given set of physical parameters is determined by the relation between the two ratios $\gamma_m/\widehat{\gamma_m}$ and ϵ_e/ϵ_B. The shape of the spectrum also depends on the value of γ_c relatively to the other critical frequencies. Moreover, the time evolution of γ_c depends on its relative value. In this section, we assume that in each of the subcases γ_c is small and has no significant effect on the spectrum above ν_c. The effects of γ_c on the spectra in the different cases and its evolution are discussed in Section 5.

The SSC spectrum in this regime includes too many subcases and power-law segments to list them all in a useful way. However, the differences between the power-law indices of the various segments is typically small ($\leqslant 1/4$). Therefore for each subcase below we give a rough description of the SSC spectrum, mostly near $\nu_{\rm peak}^{\rm IC}$, which is accurate enough for comparison with observation. A common feature of the SSC spectra in this regime ($\gamma_c, \widehat{\gamma_m} < \gamma_m$) is that most of the SSC energy is radiated by γ_m electrons at $\nu_{\rm peak}^{\rm IC} \approx 2\nu_m\gamma_m\widehat{\gamma_m}$.

Before discussing the specific subcases it is useful to note that in this regime γ_m electrons do not upscatter their own synchrotron photons and therefore we cannot easily determine $Y(\gamma_m)$. However, since in this regime $\nu_{\rm self} < \nu_{\rm peak}^{\rm syn}$ electrons with Lorentz factor $\gamma_{\rm self}$ are primarily cooling on their own emitted synchrotron photons (assuming $\gamma_c < \gamma_{\rm self}$). The total luminosity emitted by electrons with Lorentz factor of order γ is proportional to $\gamma N_\gamma(d\gamma/dt)$, and is therefore independent of Y and proportional to γ for $\gamma_c < \gamma < \gamma_m$ (see Equations (9) and (12)). Therefore, based on the discussion below Equation (3),

we can determine the value of $Y(\gamma_{\rm self})$

$$Y(\gamma_{\rm self})\,[1+Y(\gamma_{\rm self})] \approx \frac{\epsilon_e}{\epsilon_B}\frac{\gamma_{\rm self}}{\gamma_m} = \frac{\epsilon_e}{\epsilon_B}\left(\frac{\widehat{\gamma_m}}{\gamma_m}\right)^{1/3}. \quad (26)$$

3.2.1. Case IIa: $\gamma_0 < \gamma_{\rm self} < \gamma_m \left[\frac{\epsilon_e}{\epsilon_B} < \left(\frac{\gamma_m}{\widehat{\gamma_m}}\right)^{1/3}\right]$

Since γ_0 is smaller than $\widehat{\gamma_0}$, $\widehat{\widehat{\gamma_m}}$ and $\widehat{\gamma_c}$, synchrotron breaks (in addition to ν_m and ν_c) correspond only to $\widehat{\gamma_m}$ and γ_0. Electrons with $\gamma > \gamma_0$ cool by synchrotron emission implying $F_\nu(\nu_0 < \nu < \nu_m) \propto \nu^{-1/2}$ and $\alpha(\widetilde{\gamma}) = -1/2$ for electrons with $\widehat{\gamma_m} < \gamma < \widehat{\gamma_0}$. It follows that $Y(\widehat{\gamma_m} < \gamma < \widehat{\gamma_0}) \propto \gamma^{-1/2}$ and from Equations (12) and (18), $F_\nu(\widehat{\nu_m} < \nu < \nu_0) \propto \nu^{-1/4}$. As $\widehat{\gamma_m} < \gamma_0, \gamma_{\rm self} < \widehat{\gamma_0}$ we can use Equation (26) to find

$$\gamma_0 \approx \widehat{\gamma_m}\left(\frac{\epsilon_e}{\epsilon_B}\right)^2. \quad (27)$$

The modified synchrotron spectrum implies $Y(\widehat{\gamma_0} < \gamma < \widehat{\widehat{\gamma_m}}) \propto \gamma^{-3/4}$ (note that $Y < 1$ in this range). Finally, the value of $Y(\gamma < \widehat{\gamma_m}) = \epsilon_e/\epsilon_B$ is constant since these electrons are cooling on ν_m photons which are emitted by γ_m electrons that are predominantly cooling by synchrotron radiation. The complete spectrum is therefore

$$Y(\gamma) \approx \begin{cases} \frac{\epsilon_e}{\epsilon_B} & \gamma < \widehat{\gamma_m} \\ \frac{\epsilon_e}{\epsilon_B}\left(\frac{\gamma}{\widehat{\gamma_m}}\right)^{-1/2} & \widehat{\gamma_m} < \gamma < \frac{\gamma_m^2}{\widehat{\gamma_m}}\left(\frac{\epsilon_e}{\epsilon_B}\right)^{-4} \\ \widehat{\gamma_m}^{1/4}\gamma_m^{1/2}\gamma^{-3/4} & \frac{\gamma_m^2}{\widehat{\gamma_m}}\left(\frac{\epsilon_e}{\epsilon_B}\right)^{-4} < \gamma < \frac{\gamma_m^2}{\widehat{\gamma_m}} \\ \widehat{\gamma_m}^{1/2}\gamma^{-1/2} & \frac{\gamma_m^2}{\widehat{\gamma_m}} < \gamma \end{cases}, \quad (28)$$

and the synchrotron spectrum is modified only between $\widehat{\nu_m}$ and ν_0:

$$F_\nu^{\rm syn} \propto \begin{cases} \nu^{-1/2} & \nu_c < \nu < \widehat{\nu_m} \\ \nu^{-1/4} & \widehat{\nu_m} < \nu < \nu_0 \\ \nu^{-1/2} & \nu_0 < \nu < \nu_m \\ \nu^{-p/2} & \nu_m < \nu. \end{cases} \quad (29)$$

SSC spectrum. Most of the SSC energy is radiated by γ_m electrons that upscatter synchrotron photons emitted by electrons with $\widetilde{\gamma_m} = \gamma_m^{1/2}\widehat{\gamma_m}^{1/2}$. Therefore, the peak of $\nu F_\nu^{\rm IC}$ is at $\nu_{\rm peak}^{\rm IC} \sim 2\nu_m\gamma_m\widehat{\gamma_m}$. The SSC power-law index (of $F_\nu^{\rm IC}$) at frequencies just below $\nu_{\rm peak}^{\rm IC}$ can range between $-1/2$ and $-3/4$. At much lower frequencies it can be as shallow as $-1/4$. At $\nu > \nu_{\rm peak}^{\rm IC}$ the power-law index range between $-p+1/2$ and $-p+1/4$, where at higher frequencies ($\nu > 2\nu_c\widehat{\gamma_c}^2$) the index becomes $-p-1/3$.

An example of a Case IIa analytic synchrotron-SSC spectrum and comparison to the numerical spectrum is presented in Figure 2. The normalization of the analytic SSC spectrum is calculated using Equation (42).

3.2.2. Case IIb: $\widehat{\gamma_m} < \gamma_{\rm self} < \gamma_0 < \gamma_m \left[\left(\frac{\gamma_m}{\widehat{\gamma_m}}\right)^{1/3} < \frac{\epsilon_e}{\epsilon_B} < \frac{\gamma_m}{\widehat{\gamma_m}}\right]$

In addition to ν_c and ν_m, the break frequencies in this case correspond to $\widehat{\gamma_m}$, $\widehat{\gamma_0}$, and γ_0. $\widehat{\widehat{\gamma_0}}$, $\widehat{\widehat{\gamma_m}}$, and $\widehat{\gamma_c}$ are all larger than γ_0 and therefore do not affect the electron distribution (note that we assume $\gamma_c < \widehat{\gamma_m}$). Here, $\gamma_{\rm self}$ electrons are cooling primarily by their own synchrotron photons and $\nu_{\rm self} < \nu_{\rm peak}^{\rm syn}$. As a result, a new power-law segment is introduced. Plugging Equation (16) into Equation (12) using $\gamma_{\rm self} = \widetilde{\gamma_{\rm self}}$, we get $N_\gamma(\gamma_{\rm self}) \propto \gamma^{\alpha(\gamma_{\rm self})-1}$, which according to Equation (17) implies $\alpha(\gamma_{\rm self}) = 0$. Therefore, $\alpha(\widehat{\gamma_0} < \gamma < \gamma_0) = 0$ and $Y(\widehat{\gamma_0} < \gamma < \widehat{\widehat{\gamma_0}}) \propto \gamma^{-1}$ implying:

$$\gamma_0 \approx \sqrt{\frac{\epsilon_e}{\epsilon_B}\gamma_m\widehat{\gamma_m}}. \quad (30)$$

Additional power-law segments are $Y(\widehat{\gamma_m} < \gamma < \widehat{\gamma_0}) \propto \gamma^{-1/2}$ and $\alpha(\widehat{\gamma_m} < \gamma < \widehat{\gamma_0}) = -1/4$, where the latter implies $Y(\widehat{\widehat{\gamma_m}} < \gamma < \widehat{\widehat{\gamma_0}}) \propto \gamma^{-3/4}$. Similar to the previous case, $Y(\gamma < \widehat{\gamma_m}) = \epsilon_e/\epsilon_B$ since $Y(\gamma_m) < 1$. The resulting Y spectrum is therefore

$$Y(\gamma) \approx \begin{cases} \frac{\epsilon_e}{\epsilon_B} & \gamma < \widehat{\gamma_m} \\ \frac{\epsilon_e}{\epsilon_B}\left(\frac{\gamma}{\widehat{\gamma_m}}\right)^{-1/2} & \widehat{\gamma_m} < \gamma < \gamma_m\left(\frac{\epsilon_e}{\epsilon_B}\right)^{-1} \\ \left(\frac{\epsilon_e}{\epsilon_B}\right)^{1/2}\widehat{\gamma_m}^{1/2}\gamma_m^{1/2}\gamma^{-1} & \gamma_m\left(\frac{\epsilon_e}{\epsilon_B}\right)^{-1} < \gamma < \widehat{\gamma_m}\left(\frac{\epsilon_e}{\epsilon_B}\right)^2. \\ \gamma_m^{1/2}\widehat{\gamma_m}^{1/4}\gamma^{-3/4} & \widehat{\gamma_m}\left(\frac{\epsilon_e}{\epsilon_B}\right)^2 < \gamma < \frac{\gamma_m^2}{\widehat{\gamma_m}} \\ \widehat{\gamma_m}^{1/2}\gamma^{-1/2} & \frac{\gamma_m^2}{\widehat{\gamma_m}} < \gamma \end{cases} \quad (31)$$

The synchrotron spectrum in this case is affected only between $\widehat{\nu}$ and ν_0:

$$F_\nu^{\rm syn} \propto \begin{cases} \nu^{-1/2} & \nu_c < \nu < \widehat{\nu_m} \\ \nu^{-1/4} & \widehat{\nu_m} < \nu < \widehat{\nu_0} \\ \nu^0 & \widehat{\nu_0} < \nu < \nu_0 \\ \nu^{-1/2} & \nu_0 < \nu < \nu_m \\ \nu^{-p/2} & \nu_m < \nu \end{cases}. \quad (32)$$

SSC spectrum. Similarly to the previous case, $\nu_{\rm peak}^{\rm IC} \sim 2\nu_m\gamma_m\widehat{\gamma_m}$. Just below the peak, the spectral index is $-3/4$ down to $\sqrt{\frac{\widehat{\gamma_m}\epsilon_e}{\gamma_m\epsilon_B}}\nu_{\rm peak}^{\rm IC}$ where it becomes $-1/4$.[6] Above the peak the power-law index ranges between $-p$ and $-p+1/4$, where at higher frequencies it becomes $-p+1/2$ and at even higher frequencies ($\nu > 2\nu_c\widehat{\gamma_c}^2$) it is $-p-1/3$.

An example of the analytic Case IIb synchrotron-SSC spectrum and comparison to the numerical spectrum is presented in Figure 3. The normalization of the analytic SSC spectrum is calculated using Equation (42).

3.2.3. Case IIc: $\widehat{\gamma_m} < \gamma_{\rm self} < \gamma_m < \gamma_0 < \widehat{\widehat{\gamma_m}}\left[\frac{\gamma_m}{\widehat{\gamma_m}} < \frac{\epsilon_e}{\epsilon_B} < \left(\frac{\gamma_m}{\widehat{\gamma_m}}\right)^3\right]$

Under these assumptions, the critical Lorentz factors are $\widehat{\gamma_m}$, $\widehat{\gamma_0}$, and γ_0 (similar to Case IIb). In this case, $\widehat{\gamma_0} < \widehat{\gamma_m}$ and therefore $Y(\gamma) \propto \gamma^{-1}$ for $\widehat{\gamma_m} < \gamma < \widehat{\widehat{\gamma_m}}$. Similar to the previous case

$$\gamma_0 \approx \sqrt{\frac{\epsilon_e}{\epsilon_B}\gamma_m\widehat{\gamma_m}}. \quad (33)$$

[6] For very large values of $\epsilon_e/\epsilon_B > 10^5$ it can approach 0 before it return to $-1/4$.

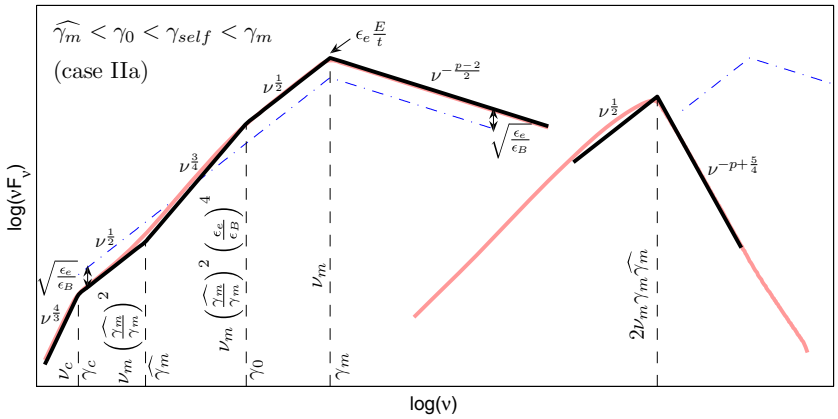

Figure 2. Synchrotron-SSC spectrum for $\gamma_c < \widehat{\gamma_m} < \gamma_0 < \gamma_{\rm self} < \gamma_m$ (Case IIa). The specific parameters are $\gamma_m/\widehat{\gamma_m} = 10^{11}$, $\epsilon_e/\epsilon_B = 10^3$ and $p = 2.4$. The notations are similar to Figure 1.

(A color version of this figure is available in the online journal.)

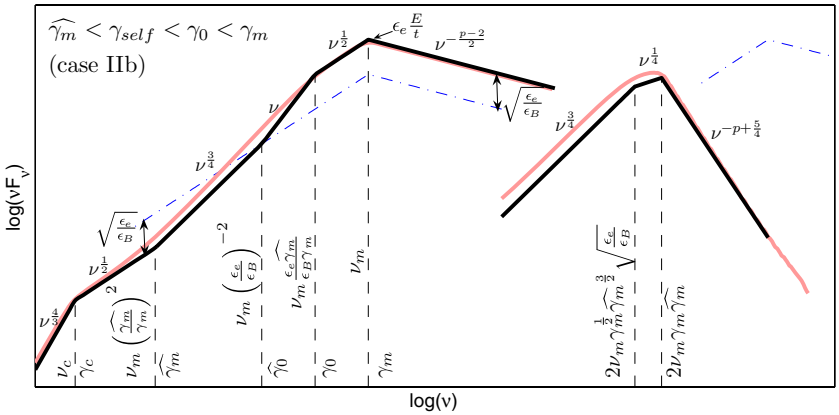

Figure 3. Synchrotron-SSC spectrum for $\gamma_c < \widehat{\gamma_m} < \gamma_{\rm self} < \gamma_0 < \gamma_m$ (Case IIb). The specific parameters are $\gamma_m/\widehat{\gamma_m} = 10^8$, $\epsilon_e/\epsilon_B = 10^4$, and $p = 2.4$. The notations are similar to Figure 1.

(A color version of this figure is available in the online journal.)

Since $\gamma_m < \gamma_0$, the synchrotron power-law index above ν_m is modified from $p/2$ to $(p-1)/2$ up to ν_0, implying that if $2 < p < 3$, then $\nu^{\rm syn}_{\rm peak} \approx \nu_0$ and as a result $Y(\gamma) \propto \gamma^{(p-3)/2}$ for $\widehat{\gamma_0} < \gamma < \widehat{\gamma_m}$. Note that γ_0 electrons carry a fraction $\approx (\gamma_0/\gamma_m)^{2-p}$ of the total electrons energy which they radiate entirely as synchrotron photons. Therefore, the maximal value of Y when synchrotron emissivity is dominated by γ_0 electrons (i.e., $p < 3$) is $Y(\widehat{\gamma_0}) \approx \frac{\epsilon_e}{\epsilon_B}\left(\frac{\gamma_0}{\gamma_m}\right)^{2-p}$. Thus, the Y spectrum in case that $2 < p < 3$ is

$$Y(\gamma) \approx \begin{cases} \left(\frac{\epsilon_e}{\epsilon_B}\right)^{\frac{4-p}{2}} \left(\frac{\widehat{\gamma_m}}{\gamma_m}\right)^{\frac{2-p}{2}} & \gamma < \gamma_m \left(\frac{\epsilon_e}{\epsilon_B}\right)^{-1} \\ \left(\frac{\epsilon_e}{\epsilon_B}\right)^{\frac{1}{2}} \gamma_m^{1/2} \widehat{\gamma_m}^{\frac{2-p}{2}} \gamma^{-\frac{3-p}{2}} & \gamma_m \left(\frac{\epsilon_e}{\epsilon_B}\right)^{-1} < \gamma < \widehat{\gamma_m} \\ \left(\frac{\epsilon_e}{\epsilon_B}\right)^{\frac{1}{2}} \widehat{\gamma_m}^{1/2} \gamma_m^{1/2} \gamma^{-1} & \widehat{\gamma_m} < \gamma < \frac{\gamma_m^2}{\widehat{\gamma_m}} \\ \left(\frac{\epsilon_e}{\epsilon_B}\right)^{\frac{1}{2}} \widehat{\gamma_m}^{\frac{p+1}{4}} \gamma_m^{\frac{2-p}{2}} \gamma^{-\frac{5-p}{4}} & \frac{\gamma_m^2}{\widehat{\gamma_m}} < \gamma < \left(\frac{\epsilon_e}{\epsilon_B}\right)^2 \widehat{\gamma_m} \\ \left(\frac{\epsilon_e}{\epsilon_B}\right)^{\frac{p-2}{2}} \widehat{\gamma_m}^{\frac{p-1}{2}} \gamma_m^{\frac{2-p}{2}} \gamma^{-1/2} & \left(\frac{\epsilon_e}{\epsilon_B}\right)^2 \widehat{\gamma_m} < \gamma. \end{cases} \quad (34)$$

The synchrotron spectrum in this case is affected only between $\widehat{\nu_0}$ and ν_0:

$$F_\nu^{\rm syn} \propto \begin{cases} \nu^{-\frac{1}{2}} & \nu_c < \nu < \widehat{\nu_0} \\ \nu^{-\frac{p-1}{4}} & \widehat{\nu_0} < \nu < \widehat{\nu_m} \\ \nu^0 & \widehat{\nu_m} < \nu < \nu_m \\ \nu^{-\frac{p-1}{2}} & \nu_m < \nu < \nu_0 \\ \nu^{-\frac{p}{2}} & \nu_0 < \nu. \end{cases} \quad (35)$$

In case that $p > 3$, most of the synchrotron energy is emitted at ν_m, eliminating the second and fourth power-law segments in Equation (34). Instead, $Y(\gamma < \widehat{\gamma_m}) = [(\epsilon_e\gamma_m)/(\epsilon_B\widehat{\gamma_m})]^{1/2}$ and $Y(\gamma > \gamma_m^2/\widehat{\gamma_m}) \propto \gamma^{-1/2}$. Equation (35) is then revised so $F_\nu \propto \nu^{1/2}$ for all $\nu_c < \nu < \nu_m(\widehat{\gamma_m}/\gamma_m)^2$.

If $\widehat{\widehat{\gamma_m}} < \gamma_0$, then $\widehat{\widehat{\gamma_m}}$ becomes a new critical lorentz factor and two more power-law segments are added, slightly modifying Equations (34)–(35). Yet more power-law segments are added if $\widehat{\widehat{\widehat{\gamma_m}}} < \gamma_0$ and so on. Asymptotically, the spectrum approaches the case where $\gamma_m = \widehat{\gamma_m}$ which we solve next (Case III). Moreover, the criterion for $\widehat{\widehat{\gamma_m}} < \gamma_0$ is $\gamma_m/\widehat{\gamma_m} < (\epsilon_e/\epsilon_B)^{1/3}$ which for most typical values of (ϵ_e/ϵ_B) implies $\gamma_m/\widehat{\gamma_m} \lesssim 10$ and therefore this case (as well as all higher order cases) is well approximated by Case III.

SSC spectrum. Similar to the two previous cases, $\nu^{\rm IC}_{\rm peak} \sim \nu_m\gamma_m\widehat{\gamma_m}$. The spectral index below the peak ranges between

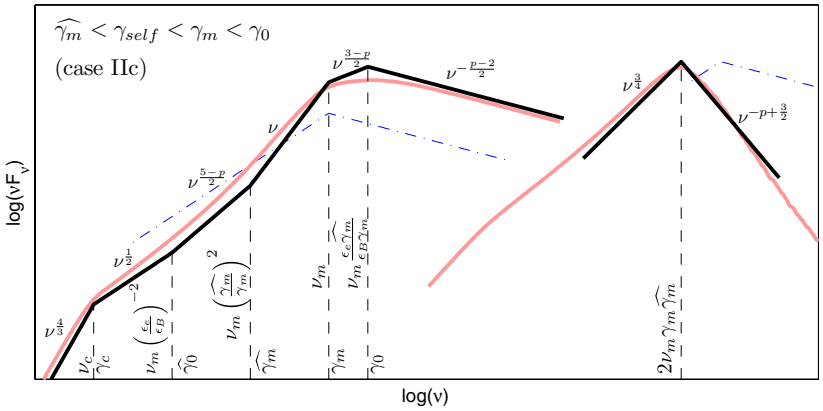

Figure 4. Synchrotron-SSC spectrum for $\gamma_c < \widehat{\gamma_m} < \gamma_{\rm self} < \gamma_m < \gamma_0$ (Case IIc). The specific parameters are $\gamma_m/\widehat{\gamma_m} = 10^2$, $\epsilon_e/\epsilon_B = 10^4$, and $p = 2.4$. The notations are similar to Figure 1.

(A color version of this figure is available in the online journal.)

$-1/4$ and 0 (where the latter can be observed only for very large values of $\epsilon_e/\epsilon_B > 10^5$) and above the peak it ranges between $-p$ and $-p+1/2$ where at higher frequencies ($\nu > 2\nu_c\widehat{\gamma_c}^2$) it becomes $-p-1/3$.

An example of the analytic Case IIc synchrotron-SSC spectrum and comparison to the numerical spectrum is presented in Figure 4. The normalization of the analytic SSC spectrum is calculated using Equation (42).

3.3. Case III—$\gamma_m = \widehat{\gamma_m}$

Here, $\gamma_m = \widehat{\gamma_m} = \widehat{\widehat{\gamma_m}} = \cdots$ and therefore γ_0 and potentially $\widehat{\gamma_0}$ are the only critical Lorentz factors in addition to γ_c and γ_m. As we show below there is a slight difference between cases where $p < 2.5$, for which $\nu^{\rm syn}_{\rm peak} = \nu_0$, and spectra with $p > 2.5$ where $\nu^{\rm syn}_{\rm peak} = \nu_m$. In both cases, electrons with $\gamma_m < \gamma < \gamma_0$ are cooling predominantly by upscattering photons with $\nu < \nu_m$ but if $\nu^{\rm syn}_{\rm peak} = \nu_0$ then electrons with $\gamma < \gamma_m$ are cooling by upscattering $\nu > \nu_m$ photons while if $\nu^{\rm syn}_{\rm peak} = \nu_m$ then they are cooling by upscattering ν_m photons. Solving for the mutual dependence of the spectral slopes above and below ν_m on each other in case that $\nu^{\rm syn}_{\rm peak} = \nu_0$ (using Equations (12), (16), and (18)) results in $\alpha(\widehat{\gamma_0} < \gamma < \gamma_m) = (1-p)/3$ and $\alpha(\gamma_m < \gamma < \gamma_0) = 2(1-p)/3$ (see also Pe'er & Waxman 2005a). This result shows that the transition from $\nu^{\rm syn}_{\rm peak} = \nu_0$ to $\nu^{\rm syn}_{\rm peak} = \nu_m$ takes place at $p = 2.5$.

Therefore if $p < 2.5$ then

$$\gamma_0 = \gamma_m(\epsilon_e/\epsilon_B)^{\frac{3}{2(4-p)}}; \quad p < 2.5. \tag{36}$$

The Y spectrum is

$$Y(\gamma) \approx \begin{cases} \left(\frac{\epsilon_e}{\epsilon_B}\right)^{\frac{1}{2}+\frac{5-2p}{4-p}} & \gamma < \gamma_m\left(\frac{\epsilon_e}{\epsilon_B}\right)^{-\frac{3}{4-p}} \\ \left(\frac{\epsilon_e}{\epsilon_B}\right)^{\frac{1}{2}}\left(\frac{\gamma}{\gamma_m}\right)^{-\frac{5-2p}{3}} & \gamma_m\left(\frac{\epsilon_e}{\epsilon_B}\right)^{-\frac{3}{4-p}} < \gamma < \gamma_m \\ \left(\frac{\epsilon_e}{\epsilon_B}\right)^{\frac{1}{2}}\left(\frac{\gamma}{\gamma_m}\right)^{-\frac{4-p}{3}} & \gamma_m < \gamma < \gamma_m\left(\frac{\epsilon_e}{\epsilon_B}\right)^{-\frac{6}{4-p}} \\ & p < 2.5, \\ \left(\frac{\epsilon_e}{\epsilon_B}\right)^{\frac{3(p-2)}{2(4-p)}}\left(\frac{\gamma}{\gamma_m}\right)^{-\frac{1}{2}} & \gamma_m\left(\frac{\epsilon_e}{\epsilon_B}\right)^{\frac{6}{4-p}} < \gamma < \widehat{\gamma_c} \end{cases}; \tag{37}$$

the synchrotron spectrum is

$$F^{\rm syn}_\nu \propto \begin{cases} \nu^{-\frac{1}{2}} & \nu_c < \nu < \widehat{\nu_0} \\ \nu^{-\frac{p-1}{3}} & \widehat{\nu_0} < \nu < \nu_m; \\ \nu^{-\frac{2(p-1)}{3}} & \nu_m < \nu < \nu_0 \\ \nu^{-\frac{p}{2}} & \nu_0 < \nu \end{cases} \quad p < 2.5, \tag{38}$$

and the SSC spectrum is

$$F^{\rm IC}_\nu \propto \begin{cases} \nu^{-\frac{1}{2}} & 2\nu_m\gamma_c^2 < \nu < 2\nu_m\widehat{\gamma_0}^2 \\ \nu^{-\frac{p-1}{3}} & 2\nu_m\widehat{\gamma_0}^2 < \nu < 2\nu_m\gamma_m^2 \\ \nu^{-p+1} & 2\nu_m\gamma_m^2 < \nu < 2\nu_m\gamma_m\gamma_0; \\ \nu^{-\frac{2p+1}{3}} & 2\nu_m\gamma_m\gamma_0 < \nu < 2\nu_m\gamma_m\widehat{\widehat{\gamma_0}} \\ \nu^{-p+\frac{1}{2}} & 2\nu_m\gamma_m\widehat{\widehat{\gamma_0}} < \nu \end{cases} \quad p < 2.5. \tag{39}$$

In case that $p > 2.5$, then Equation (37) can be used by substituting $p \to 2.5$. The synchrotron spectrum (Equation (38)) is modified so the spectral index at $\nu_c < \nu < \nu_m$ is $-1/2$ and at $\nu_m < \nu < \nu_0$ it is $-p/2+1/4$, where $\gamma_0 = \gamma_m(\epsilon_e/\epsilon_B)$. The spectral index of SSC spectrum at $2\nu_c\gamma_c^2 < \nu < 2\nu_m\gamma_m^2$ is $-1/2$, at $2\nu_m\gamma_m^2 < \nu < 2\nu_m\gamma_m\gamma_0$ it is $-p+1$ and at $\nu > 2\nu_m\gamma_m\gamma_0$ it is $-p+1/2$.

An example of the analytic Case III synchrotron-SSC spectrum with $p < 2.5$ and comparison to the numerical spectrum is presented in Figure 5. The normalization of the analytic SSC spectrum is calculated using Equation (42).

3.4. The Dependence of the SSC to Synchrotron Luminosity Ratio on $\gamma_m/\widehat{\gamma_m}$

The SSC to synchrotron luminosity ratio is an observable that can be used in order to constrain the physical parameters of the source. Here, we derive this ratio as a function of $\gamma_m/\widehat{\gamma_m}$, where the rest of the physical parameters (e.g., ϵ_e/ϵ_B) are held constant and $\gamma_c \ll \gamma_m, \widehat{\gamma_m}$, so the value of γ_c do not affect the results. The SSC to synchrotron luminosity ratio is an average of $Y(\gamma)$ weighted by the synchrotron emissivity

$$\overline{Y} \equiv \frac{L_{\rm IC}}{L_{\rm syn}} = \frac{\int YP_{\rm syn}N_\gamma d\gamma}{\int P_{\rm syn}N_\gamma d\gamma}. \tag{40}$$

In case, where KN effects can be neglected then Y is a constant and $\overline{Y} = Y_{\rm noKN}$ (see Equations (2) and (3)). The

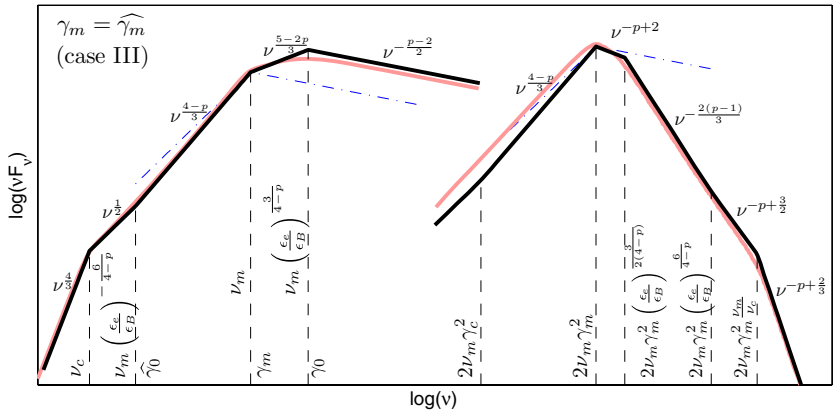

Figure 5. Synchrotron-SSC spectrum for $\gamma_c < \widehat{\gamma_m} = \gamma_m$ (Case III). The specific parameters are $\epsilon_e/\epsilon_B = 10^3$ and $p = 2.2$. The notations are similar to Figure 1.
(A color version of this figure is available in the online journal.)

SSC luminosity is dominated by γ_m electrons. Typically, the synchrotron luminosity is dominated by γ_m electrons as well in which case $\overline{Y} \approx Y(\gamma_m)$. The value $Y(\gamma_m)$ is also of interest since there are cases where $F_{\nu,\rm syn}(\gamma_m)$ is the observable. Therefore, we first find $Y(\gamma_m)$.

The dependence of $Y(\gamma_m)$ on the ratio $\gamma_m/\widehat{\gamma_m}$ can be approximated using Equations (28), (31), and (34). For $\gamma_m/\widehat{\gamma_m} \ll 1$, there is no significant KN effect and $Y(\gamma_m) \approx (\epsilon_e/\epsilon_B)^{1/2}$. When $\gamma_m/\widehat{\gamma_m} \approx 1$, the energy in γ_m electrons is roughly a fraction of $\approx p-2$ out of the total energy in electrons and therefore $Y(\gamma_m) \approx [(p-2)\epsilon_e/\epsilon_B]^{1/2}$. For $\gamma_m/\widehat{\gamma_m} \lesssim 1$ (Case IIc) and $\gamma_m/\widehat{\gamma_m} \ll 1$ (part of Case IIa), one obtains $Y(\gamma_m) \propto (\gamma_m/\widehat{\gamma_m})^{-1/2}$, with a slightly different dependence ($\propto (\gamma_m/\widehat{\gamma_m})^{-1/4}$) for intermediate values of $\gamma_m/\widehat{\gamma_m}$. Therefore, a simple approximation for $Y(\gamma_m)$ is (Ando et al. 2008),

$$Y(\gamma_m) \approx \sqrt{\frac{\epsilon_e}{\epsilon_B}} \begin{cases} 1 & \dfrac{\gamma_m}{\widehat{\gamma_m}} < p-2 \\ \sqrt{p-2}\left(\dfrac{\gamma_m}{\widehat{\gamma_m}}\right)^{-1/2} & \dfrac{\gamma_m}{\widehat{\gamma_m}} > p-2. \end{cases} \quad (41)$$

The quality of this approximation is depicted in Figure 6. It is accurate to within a factor of ≈ 2 as long as $\gamma_m/\widehat{\gamma_m} < (\epsilon_e/\epsilon_B)^2$ or for any reasonable value of $\gamma_m/\widehat{\gamma_m}$ when $\epsilon_e/\epsilon_B \lesssim 100$. A more accurate approximation which includes the intermediate segment of $Y \propto \gamma^{-1/4}$ and should be used for large values of ϵ_e/ϵ_B is

$$Y(\gamma_m) \approx \begin{cases} \sqrt{\dfrac{\epsilon_e}{\epsilon_B}} & \dfrac{\gamma_m}{\widehat{\gamma_m}} < p-2 \\ \sqrt{\dfrac{(p-2)\epsilon_e}{\epsilon_B}}\left(\dfrac{\gamma_m}{\widehat{\gamma_m}}\right)^{-1/2} & p-2 < \dfrac{\gamma_m}{\widehat{\gamma_m}} < \left(\dfrac{\epsilon_e}{\epsilon_B}\right)^2 \\ \sqrt{p-2}\left(\dfrac{\gamma_m}{\widehat{\gamma_m}}\right)^{-1/4} & \left(\dfrac{\epsilon_e}{\epsilon_B}\right)^2 < \dfrac{\gamma_m}{\widehat{\gamma_m}} < \left(\dfrac{\epsilon_e}{\epsilon_B}\right)^4 \\ \sqrt{p-2}\dfrac{\epsilon_e}{\epsilon_B}\left(\dfrac{\gamma_m}{\widehat{\gamma_m}}\right)^{-1/2} & \left(\dfrac{\epsilon_e}{\epsilon_B}\right)^4 < \dfrac{\gamma_m}{\widehat{\gamma_m}}. \end{cases} \quad (42)$$

The approximation $\overline{Y} \approx Y(\gamma_m)$ is good as long as the synchrotron luminosity peaks at ν_m. This is not the case when $p < 2.5$ and $(\epsilon_e/\epsilon_B)^{((p-2.5)/(p-2))} < \gamma_m/\widehat{\gamma_m} < \epsilon_e/\epsilon_B$, where the synchrotron luminosity is dominated by γ_0 electrons and

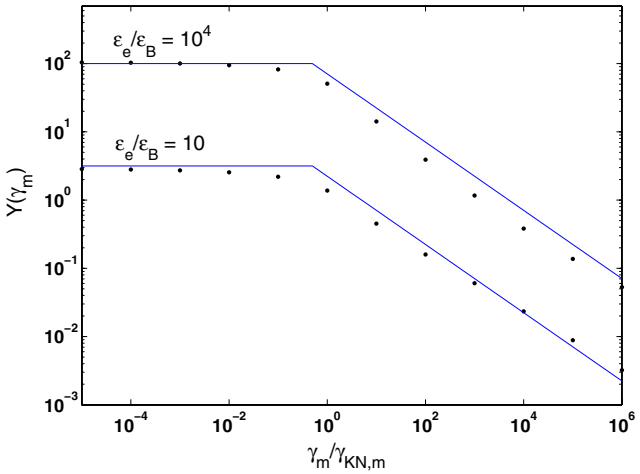

Figure 6. Value of $Y(\gamma_m)$ as calculated numerically by integrating Equations (9), (10), and (15) (dots) compared to the simple approximation of Equation (41) (solid lines) for two values of ϵ_e/ϵ_B and $p = 2.5$.
(A color version of this figure is available in the online journal.)

$\overline{Y} \approx Y(\gamma_m)L_{\rm syn}(\gamma_m)/L_{\rm syn}(\gamma_0)$ (note that the SSC luminosity is dominated by γ_m electrons also in this regime). Since $\gamma_0 \approx \gamma_m(\epsilon_e/\epsilon_B)$ for $\gamma_m < \widehat{\gamma_m}$, a reasonably simple approximation for $\overline{Y}$ is

$$\overline{Y} \approx \begin{cases} \left(\dfrac{\epsilon_B\gamma_m}{\epsilon_e\widehat{\gamma_m}}\right)^{p-2} & \text{if } \left(\dfrac{\epsilon_e}{\epsilon_B}\right)^{-\frac{2.5-p}{p-2}} < \dfrac{\gamma_m}{\widehat{\gamma_m}} < \dfrac{\epsilon_e}{\epsilon_B}(p-2)^{\frac{1}{2(2.5-p)}} \\ & \text{and } p < 2.5 \\ Y(\gamma_m) & \text{otherwise.} \end{cases} \quad (43)$$

Figure 7 shows this approximation for large value of $\epsilon_e/\epsilon_B = 10^4$ and $p = 2.1$, where the approximation $\overline{Y} = Y(\gamma_m)$ is not adequate. Equation (43) provides a reasonable approximation that is accurate only to within an order of magnitude. The largest deviation of Equation (43) is in the range $\widehat{\gamma_m} < \gamma_m < \widehat{\gamma_m}(\epsilon_e/\epsilon_B)$ where it can overestimate the value of $\overline{Y}$ by an order of magnitude.

3.5. Dominant Synchrotron Cooling [$\epsilon_e \lesssim \epsilon_B$]

Since only the electrons' energy can be radiated, $U_{\rm ph} < \epsilon_e U$. Therefore, $\epsilon_e < \epsilon_B$ guarantees that the magnetic field energy density is larger than the synchrotron photon energy density,

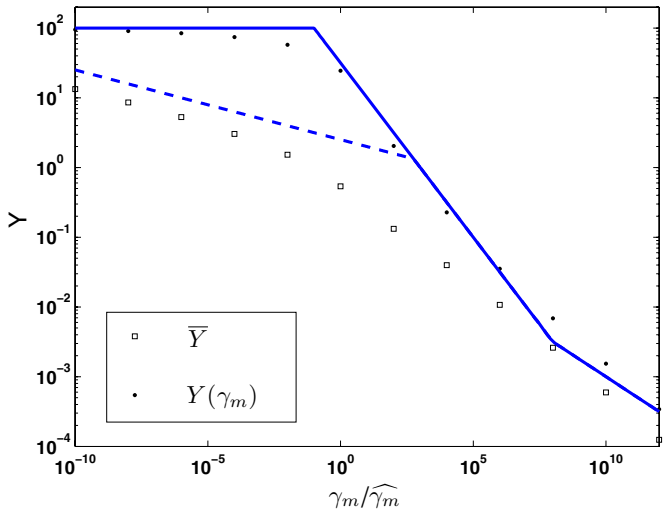

Figure 7. Value of $\overline{Y}$ (open squares) and $Y(\gamma_m)$ (dots) as calculated numerically (by integrating Equations (9), (10), and (15)), compared to the analytic approximation Equation (43; dashed lines) and Equation (42; solid lines). The parameters are $p = 2.1$ and $\epsilon_e/\epsilon_B = 10^4$.

(A color version of this figure is available in the online journal.)

and the cooling of all the electrons is dominated by synchrotron emission. In such a case, the synchrotron spectrum is not affected at all by the SSC emission. The SSC spectrum, however, is affected by the KN limit:

$$F_\nu^{\rm IC} \propto \begin{cases} \nu^{-\frac{1}{2}} & 2\nu_c\gamma_c^2 < \nu < 2\nu_m\gamma_m \min\{\gamma_m, \widehat{\gamma_m}\} \\ \nu^{-p+\frac{1}{2}} & 2\nu_m\gamma_m \min\{\gamma_m, \widehat{\gamma_m}\} < \nu < 2\nu_c\widehat{\gamma_c}^2 \\ \nu^{-(p+\frac{1}{3})} & 2\nu_c\widehat{\gamma_c}^2 < \nu. \end{cases} \quad (44)$$

The SSC to synchrotron energy output is well approximated by $Y(\gamma_m)$ and it is

$$\overline{Y} \approx Y(\gamma_m) \approx \frac{\epsilon_e}{\epsilon_B} \begin{cases} 1 & \frac{\gamma_m}{\widehat{\gamma_m}} < (p-2)^2 \\ (p-2)\left(\frac{\gamma_m}{\widehat{\gamma_m}}\right)^{-1/2} & \frac{\gamma_m}{\widehat{\gamma_m}} > (p-2)^2, \end{cases} \quad (45)$$

where we assume here $\gamma_c < \widehat{\gamma_m}$.

4. SLOW COOLING

This regime is more simple since the electron distribution is not affected by inverse-Compton (or synchrotron) cooling at $\gamma < \gamma_c$ while SSC cooling of electrons with $\gamma > \gamma_c$ is always dominated by upscattering synchrotron photons with frequency $\leqslant \nu_c$. This significantly simplifies the electron distribution. We present in this regime only the case that $\gamma_c < \widehat{\gamma_m}$ since if $\gamma_c > \widehat{\gamma_m}$ then $Y(\gamma_c) < 1$ (see Section 5) and SSC cooling has no effect on the electron distribution. We also discuss only the case of $2 < p < 3$ which implies that $\nu_{\rm peak}^{\rm syn} \gtrsim \nu_c$ (for $p > 3$ the peak frequency is in most cases, ν_m).

Under these assumptions, Y typically takes the form (see exception below):

$$Y(\gamma) = Y(\widehat{\gamma_c}) \begin{cases} 1 & \gamma < \widehat{\gamma_c} \\ \left(\frac{\gamma}{\widehat{\gamma_c}}\right)^{\frac{p-3}{2}} & \widehat{\gamma_c} < \gamma < \widehat{\gamma_m} \\ \left(\frac{\gamma_c}{\gamma_m}\right)^{p-3}\left(\frac{\gamma}{\widehat{\gamma_m}}\right)^{-\frac{4}{3}} & \widehat{\gamma_m} < \gamma. \end{cases} \quad (46)$$

The value of $Y(\widehat{\gamma_c})$ can be found by the normalization at γ_c:

$$Y(\gamma_c)[1 + Y(\gamma_c)] \approx \frac{\epsilon_e}{\epsilon_B}\left(\frac{\gamma_c}{\gamma_m}\right)^{2-p}\left(\frac{\min\{\gamma_c, \widehat{\gamma_c}\}}{\gamma_c}\right)^{\frac{3-p}{2}}. \quad (47)$$

In the case of $\gamma_c \ll \widehat{\gamma_c}$ and $Y(\gamma_c) > 1$, Equation (47) is reduced to the slow cooling value in case that KN effects are neglected, $Y = (\epsilon_e/\epsilon_B)^{1/2}(\gamma_c/\gamma_m)^{(2-p)/2}$ (e.g., Sari & Esin 2001). Equation (47) can be used also to find γ_c when KN effects play an important role (see Section 5).

The synchrotron spectrum above ν_c is

$$F_\nu^{\rm syn} \propto \begin{cases} \nu^{-p/2} & \nu_c < \nu < \widehat{\nu_c} \\ \nu^{-\frac{3}{4}(p-1)} & \max\{\widehat{\nu_c}, \nu_c\} < \nu < \min\{\widehat{\nu_m}, \nu_0\} \\ \nu^{-(p/2-2/3)} & \widehat{\nu_m} < \nu < \nu_0; \text{ only if } \widehat{\gamma_m} < \gamma_0 \\ \nu^{-p/2} & \nu_0 < \nu, \end{cases} \quad (48)$$

Since the spectrum is altered only at $\nu > \max\{\nu_c, \nu_0\}$, not all these segments exist in all cases. For example, the first power-law segment can be observed only if $\gamma_c < \widehat{\gamma_c}$ while the third segments can be observed only if $\widehat{\gamma_m} < \gamma_0$. The value of γ_0 can be calculated using Equations (46) and (47). We give here the value of γ_0 for the case $\gamma_c < \widehat{\gamma_c}$ which is most likely to have an observable signature:

$$\gamma_0 = \begin{cases} \widehat{\gamma_c}\left(\frac{\gamma_c}{\gamma_m}\right)^{\frac{p-2}{3-p}}\left(\frac{\epsilon_e}{\epsilon_B}\right)^{\frac{1}{3-p}} & \frac{\epsilon_e}{\epsilon_B} < \left(\frac{\gamma_c}{\gamma_m}\right)^{4-p} \\ \widehat{\gamma_m}\left(\frac{\gamma_c}{\gamma_m}\right)^{\frac{3(p-4)}{8}}\left(\frac{\epsilon_e}{\epsilon_B}\right)^{\frac{3}{8}} & \frac{\epsilon_e}{\epsilon_B} > \left(\frac{\gamma_c}{\gamma_m}\right)^{4-p}, \end{cases} \quad (49)$$

where $\frac{\epsilon_e}{\epsilon_B} < \left(\frac{\gamma_c}{\gamma_m}\right)^{4-p}$ is the condition for $\gamma_0 < \widehat{\gamma_m}$.

When $p - 2 \ll 1$ and $\nu_{\rm peak}^{\rm syn} > \nu_c$, then there is another power-law segment for $Y(\gamma < \gamma_c \cdot \min\{1, \gamma_c/\widehat{\gamma_c}\})$, where $Y \propto \gamma^{(3p-7)/4}$. Yet another segment $Y \propto \gamma^{(3p-10)/2}$, corresponding to the third power-law segment in Equation (48), exists in case that the synchrotron power peaks at $\nu > \widehat{\nu_m}$. These additional segments affect only $\gamma < \gamma_c$ and therefore there is no farther effect on the electrons distribution or the synchrotron spectrum.

The KN limit affect the SSC spectrum only at $\nu > 2\nu_c\widehat{\gamma_c} \cdot \max\{\widehat{\gamma_c}, \gamma_c\}$. This regime is therefore rather similar to Case I of the fast cooling regime and the same line of reasoning we used there results in

$$F_\nu^{\rm IC} \propto \begin{cases} \nu^{-p/2} & 2\nu_c\gamma_c^2 < \nu < 2\nu_c\widehat{\gamma_c}^2 \\ \nu^{-(p-1)} & 2\nu_c\widehat{\gamma_c} \cdot \max\{\widehat{\gamma_c}, \gamma_c\} < \nu < 2\nu_c\widehat{\gamma_c} \cdot \\ & \min\{\gamma_0, \widehat{\gamma_m}\} \\ \nu^{-\frac{p+1}{2}} & 2\nu_c\widehat{\gamma_c}\gamma_0 < \nu < 2\nu_c\widehat{\gamma_c}\widehat{\gamma_m} \\ \nu^{-(p+\frac{1}{3})} & 2\nu_c\widehat{\gamma_c} \cdot \max\{\gamma_0, \widehat{\gamma_m}\} < \nu. \end{cases} \quad (50)$$

Not all these segments are always observed. The first segment is observed only when $\gamma_c < \widehat{\gamma_c}$ and the third is observed only if $\gamma_0 < \widehat{\gamma_m}$. In case that $\gamma_c < \widehat{\gamma_c}$, the total SSC luminosity is not significantly suppressed by the KN limit and the SSC peak is observed at $\nu_{\rm peak}^{\rm IC} \approx 2\nu_c\gamma_c^2$. If however, $\gamma_c > \widehat{\gamma_c}$ the SSC peak is observed at $\nu_{\rm peak}^{\rm IC} \approx 2\nu_c\gamma_c\widehat{\gamma_c}$ and the SSC luminosity (i.e., $\overline{Y}$) is suppressed. The value of $\overline{Y}$ can be approximated by $Y(\gamma_c)$ (Equation (47)) following the same reasoning explained in the fast cooling case (Section 3.4). Here, the approximation is very good for $p > 2.5$, where for lower values of p the approximation is an overestimate ($Y(\gamma_c) > \overline{Y}$) when the synchrotron luminosity is dominated by γ_0 electrons. In this case a better approximation is $\overline{Y} \approx Y(\gamma_c)L_{\rm syn}(\gamma_c)/L_{\rm syn}(\gamma_0)$, which can be calculated for a given set of parameters using Equations (46)–(48).

4.1. Dominant Synchrotron Cooling [$\epsilon_e \lesssim \epsilon_B(\gamma_m/\gamma_c)^{p-2}$]

When synchrotron cooling is dominant also in the Thomson regime then the synchrotron spectrum is not affected by IC scattering while the SSC spectrum is

$$F_\nu^{\rm IC} \propto \begin{cases} \nu^{-\frac{1}{2}} & 2\nu_m\gamma_m^2 < \nu < 2\nu_c\gamma_c \min\{\gamma_c, \widehat{\gamma_c}\} \\ \nu^{-\frac{p+1}{2}} & 2\nu_c\gamma_c \min\{\gamma_c, \widehat{\gamma_c}\} < \nu < 2\nu_m\widehat{\gamma_m}^2 \\ \nu^{-(p+\frac{1}{3})} & 2\nu_m\widehat{\gamma_m}^2 < \nu. \end{cases} \quad (51)$$

$Y(\gamma_c)$ is a good approximation of $\overline{Y}$ in this regime and it follows Equation (47).

5. THE COOLING FREQUENCY

In Sections 3 and 4, we have described the synchrotron and SSC spectra given ϵ_e/ϵ_B, γ_m, $\hat{\gamma}$, and the cooling Lorentz factor γ_c. However, the value of γ_c is also affected by the KN limit and should be solved self-consistently.[7] In this section, we show how to solve for γ_c. Moreover, we assumed before that ν_c is sufficiently low. We discuss here the modification to the spectra if ν_c is not low enough.

Electrons are cooling fast, i.e., radiating a large fraction of their initial energy over the lifetime of the system, if their Lorentz factor satisfies

$$\gamma[1 + Y(\gamma)] > \gamma_c^{\rm syn} \equiv \frac{6\pi m_e c}{\sigma_T B^2 t}, \quad (52)$$

here, $\gamma_c^{\rm syn}$ is the cooling Lorentz factor if SSC cooling is neglected altogether (e.g., Sari et al. 1998). When SSC cooling is taken into account, but KN effects are neglected $Y = Y_{\rm noKN}$ is independent of γ. Therefore, the left-hand side of the equation always increases monotonically with γ, so that $\gamma_c = \gamma_c^{\rm syn}/(1 + Y_{\rm noKN})$ is defined as a critical cooling frequency such that all electrons with $\gamma > \gamma_c$ are cooling fast and all electrons with $\gamma < \gamma_c$ are not cooling over the system lifetime. When KN effects are taken into account, Y depends on γ and since there are cases where $\gamma Y(\gamma)$ is decreasing, e.g., $Y(\gamma) \propto \gamma^{-4/3}$, the equation

$$\gamma_c[1 + Y(\gamma_c)] = \gamma_c^{\rm syn}, \quad (53)$$

has either a single solution or three different solutions. In most physical scenarios, Equation (53) has a single solution in which case the standard definition of γ_c holds, namely, γ_c is the Lorentz factor above which electrons cool over the lifetime of the system. In cases where Equation (53) has three solutions, $\gamma_{c,\rm min} < \gamma_{c,\rm mid} < \gamma_{c,\rm max}$, they satisfy $\gamma_{c,\rm min} < \gamma_{c,\rm mid} < \gamma_0 < \gamma_{c,\rm max} = \gamma_c^{\rm syn}$. Electrons with $\gamma_{c,\rm min} < \gamma < \gamma_{c,\rm mid}$ cool fast by SSC emission, electrons with $\gamma > \gamma_{c,\rm max}$ cool fast by synchrotron emission and the rest of the electrons (those with $\gamma < \gamma_{c,\rm min}$ and those with $\gamma_{c,\rm mid} < \gamma < \gamma_{c,\rm max}$) are not cooling over the system lifetime. Below, we present the solution of Equation (53) for each of the cases covered in the previous sections, and discuss the observational effects of cooling.

5.1. Fast Cooling

Case I ($\gamma_c < \gamma_m < \widehat{\gamma_m}$). The value of $Y(\gamma_c) = (\epsilon_e/\epsilon_B)^{1/2}$ is independent of γ_c and therefore

$$\gamma_c \approx \gamma_c^{\rm syn}\sqrt{\frac{\epsilon_B}{\epsilon_e}} \quad (54)$$

is a solution of Equation (53). This cooling frequency always corresponds to SSC-dominated cooling. In principle, it is possible to have three solutions to Equation (53) and thus a second synchrotron-dominated cooling frequency. However, this requires $\epsilon_e/\epsilon_B > (\widehat{\gamma_m}/\gamma_m)^8(\gamma_m/\gamma_c)^{18}$ (where γ_c is given by Equation (54)), which is unlikely to be satisfied in astrophysical sources when $\widehat{\gamma_m} \gg \gamma_m$.

Case IIa ($\widehat{\gamma_m} < \gamma_0 < \gamma_{\rm self} < \gamma_m$). In this case, Equation (53) always has a single solution and γ_c is well defined. If $\gamma_c^{\rm syn} > \gamma_0$, then $\gamma_c = \gamma_c^{\rm syn}$ and all the electrons are cooling primarily by synchrotron and therefore SSC cooling can be completely ignored. The synchrotron spectrum is then as given in, e.g., Sari et al. (1998). If $\gamma_c^{\rm syn} < \gamma_0$, electrons that are cooling by SSC, i.e., with $\gamma < \gamma_0$, are upscattering photons emitted by electrons that are cooling by synchrotron (i.e., with Lorentz factor $\widetilde{\gamma} > \gamma_0$.) In summary

$$\gamma_c \approx \gamma_c^{\rm syn}\begin{cases} 1 & \gamma_0 < \gamma_c^{\rm syn} \\ \gamma_c^{\rm syn}/\gamma_0 & (\widehat{\gamma_m}\gamma_0)^{1/2} < \gamma_c^{\rm syn} < \gamma_0 \\ \left(\dfrac{\epsilon_e}{\epsilon_B}\right)^{-1} & \gamma_c^{\rm syn} < (\widehat{\gamma_m}\gamma_0)^{1/2}. \end{cases} \quad (55)$$

If γ_c is not small enough, it affects the Compton Y-parameter in Equation (28), such that $Y(\gamma > \widehat{\gamma_c}) \propto \gamma^{-4/3}$ and affects the synchrotron spectrum in Equation (29) such that $F_\nu^{\rm syn}(\nu < \nu_c) \propto \nu^{1/3}$.

Case IIb ($\widehat{\gamma_m} < \gamma_{\rm self} < \gamma_0 < \gamma_m$). In this case, Equation (53) may have more than one solution. However, when there are three solutions, only $\gamma_{c,\rm max}$ has an observable signature. The reason is that here $\gamma_{c,\rm max} < \gamma_m$ and therefore injected electrons (all with $\gamma > \gamma_m$) do not have enough time to cool down below $\gamma_{c,\rm max}$. Thus, when there are three solutions to Equation (53), all the electrons are cooling by synchrotron emission. The transition to SSC cooling takes place when $Y(\gamma_{c,\rm max}) \approx 1$ which is also the point where $\gamma_{c,\rm max} \approx \gamma_{c,\rm mid}$ and there is transition to a single solution of Equation (53) with $\gamma_c \approx \gamma_{c,\rm min}$. We denote the value of $\gamma_{c,\rm max}$ and $\gamma_{c,\rm min}$ at this transition point as $\gamma_{c,\rm max,0}$ and $\gamma_{c,\rm min,0}$. Since $\gamma_{c,\rm min,0}$ can be much smaller than $\gamma_{c,\rm max,0}$, the observable effect of this transition is dramatic where ν_c vary on a short timescale (comparable to t) by orders of magnitude between $\nu_{\rm syn}(\gamma_{c,\rm max,0})$ and $\nu_{\rm syn}(\gamma_{c,\rm min,0})$.

The value $\gamma_{c,\rm max,0} = (\epsilon_e/\epsilon_B)^{1/3}\gamma_m^{5/9}\widehat{\gamma_m}^{4/9}$ is calculated using a synchrotron spectrum which is unaffected by SSC cooling and the requirement $Y(\gamma_{c,\rm max,0}) = 1$. (note that $\gamma_{c,\rm max,0}$ is smaller than the value of γ_0 obtained assuming $\gamma_c < \widehat{\gamma_m}$). The value of $\gamma_{c,\rm min,0}$ is calculated using Equation (31) and the requirement $\gamma_{c,\rm min,0}Y(\gamma_{c,\rm min,0}) = \gamma_{c,\rm max,0}$. If $\epsilon_e/\epsilon_B < (\gamma_m/\widehat{\gamma_m})^{5/6}$ then $\gamma_{c,\rm min,0} = (\epsilon_e/\epsilon_B)^{-4/3}\gamma_m^{10/9}\widehat{\gamma_m}^{-1/9}$, otherwise $\gamma_{c,\rm min,0} = (\epsilon_e/\epsilon_B)^{-2/3}\gamma_m^{5/9}\widehat{\gamma_m}^{4/9}$. The value of γ_c in Case IIb is therefore

$$\gamma_c \approx \gamma_c^{\rm syn}\begin{cases} 1 & \gamma_{c,\rm max,0} < \gamma_c \\ \gamma_c^{\rm syn}\widehat{\gamma_m}^{-1}\left(\dfrac{\epsilon_e}{\epsilon_B}\right)^{-2} & \widehat{\gamma_m} < \gamma_c < \gamma_{c,\rm min,0} \\ \left(\dfrac{\epsilon_e}{\epsilon_B}\right)^{-1} & \gamma_c < \min\{\widehat{\gamma_m}, \gamma_{c,\rm min,0}\}, \end{cases} \quad (56)$$

where the second segment exists only if $\epsilon_e/\epsilon_B < (\gamma_m/\widehat{\gamma_m})^{5/6}$, in which case $\widehat{\gamma_m} < \gamma_{c,\rm min,0}$. Note that γ_c cannot obtain values between $\gamma_{c,\rm max,0}$ and $\gamma_{c,\rm min,0}$.

The effect of γ_c on the observed spectrum is as follows. When $\gamma_c > \gamma_{c,\rm max,0}$ all electrons are cooling by synchrotron and the

[7] The value of γ_m is not affected by the KN limit and can be found, e.g., in Sari et al. (1998).

spectrum is therefore not affected at all by SSC and it is given by e.g., Sari et al. (1998). When $\gamma_c < \gamma_{c,\min,0}$ SSC cooling is the dominated cooling process of low-energy electrons, and Equation (31) can be used with the simple addition $Y(\gamma > \widehat{\gamma_c}) \propto \gamma^{-4/3}$. The power-law segment $F_\nu^{\rm syn}(\nu < \nu_c) \propto \nu^{1/3}$ should be added to Equation (32).

Case IIc ($\widehat{\gamma_m} < \gamma_{\rm self} < \gamma_m < \gamma_0$). The effect of the cooling frequency on the spectrum, and its behavior, are similar to the previous case (IIb). In this case, $\gamma_{c,\max,0} = (\epsilon_e/\epsilon_B)^{3/7}\gamma_m^{3/7}\widehat{\gamma_m}^{4/7}$ if $\epsilon_e/\epsilon_B > (\gamma_m/\widehat{\gamma_m})^{4/3}$ (note that $\gamma_{c,\max,0} > \gamma_m$ here). Otherwise, $\gamma_{c,\max,0} = (\epsilon_e/\epsilon_B)^{1/3}\gamma_m^{5/9}\widehat{\gamma_m}^{4/9}$. We do not give here the exact value of $\gamma_{c,\min,0}$ but in all case $\gamma_{c,\min,0} < \widehat{\gamma_m}$. When $\gamma_c > \gamma_{c,\max,0}$, all the electrons are cooling by synchrotron and there is no SSC effect while $\gamma_c < \gamma_{c,\min,0}$ implies dominant SSC cooling of all electrons with $\gamma < \gamma_0$ (including γ_m). γ_c cannot assume a value between $\gamma_{c,\min,0}$ and $\gamma_{c,\max,0}$ and the transition between $\gamma_c = \gamma_{c,\max,0}$ and $\gamma_c = \gamma_{c,\min,0}$ is observed as a sudden variation of ν_c by a few orders of magnitude on a short timescale which also accompanied by significant variation in $F_\nu(\nu_m)$ and therefore in the total synchrotron luminosity. Note that if $\gamma_{c,\max,0} > \gamma_m$, then this transition is also a transition between slow and fast cooling regimes.

Case III ($\widehat{\gamma_m} = \gamma_m$). The behavior of the cooling frequency is similar to the two previous cases with $\gamma_{c,\max,0} = \gamma_m(\epsilon_e/\epsilon_B)^{3/7}$ and $\gamma_{c,\min,0} = \gamma_m(\epsilon_e/\epsilon_B)^{-1/14}$ in case that $p > 2.5$. If $p < 2.5$, then $\gamma_{c,\max,0}$ is unchanged and $\gamma_{c,\min,0} = \gamma_m(\epsilon_e/\epsilon_B)^{-3/14/(2p-2)}$. Similar to previous cases, γ_c can vary rapidly between $\gamma_{c,\max,0}$ and $\gamma_{c,\min,0}$. Here, this transition is also a transition between slow and fast cooling regimes. In this case, there is a regime where there are three solutions to Equation (53) with $\gamma_{c,\min} < \gamma_m < \gamma_{c,\rm mid}$. In such a case, there are electrons that are cooling down to $\gamma_{c,\min}$ and there are electrons with $\gamma_{c,\rm mid} < \gamma < \gamma_{c,\max}$ that are not cooling. This regime is a short transient (unless B^2t is constant) and we do not present here the resulting spectrum.

5.2. Slow Cooling

We now describe how to find the value of γ_c in the slow cooling regime. In the following, we assume $2 < p < 3$. If $\widehat{\gamma_m} \leqslant \gamma_m$, then the system is cooling slowly if $\gamma_c^{\rm syn}$ is larger than γ_m in the Cases IIa and IIb or larger than $\gamma_{c,\max,0}$ in the Cases IIc and III. The value of γ_c is then approximately $\gamma_c^{\rm syn}$ since $Y(\gamma_c) < 1$.

If $\widehat{\gamma_m} \gg \gamma_m$ and $\epsilon_e/\epsilon_B < \widehat{\gamma_m}/\gamma_m$, then there is always a single solution to Equation (53). If $\gamma_c^{\rm syn}$ is larger than $\widehat{\gamma_m}$, then $\gamma_c = \gamma_c^{\rm syn}$. Otherwise Equation (53) should be solved where the value of $Y(\gamma_c)$ (which may still be smaller than 1) is evaluated using Equation (47).

If $\widehat{\gamma_m} \gg \gamma_m$ but $\epsilon_e/\epsilon_B > \widehat{\gamma_m}/\gamma_m$, then there may be three solutions to Equation (53) during the slow cooling phase. In this case, $\gamma_{c,\max,0} = (\epsilon_e/\epsilon_B)^{3/7}\gamma_m^{3/4}\widehat{\gamma_m}^{4/7}$ and $\gamma_{c,\min,0}$ is not much smaller than $\widehat{\gamma_m}$. Here, if $\gamma_c^{\rm syn}$ is larger than $\gamma_{c,\max,0}$ then $\gamma_c = \gamma_c^{\rm syn}$. Otherwise Equation (53) should be solved where the value of $Y(\gamma_c)$ is evaluated using Equation (47). The result then is smaller than $\widehat{\gamma_m}$. Observationally, similarly to previous cases, γ_c can vary on a short timescale between $\gamma_{c,\max,0}$ and $\gamma_{c,\min,0}$.

6. KLEIN–NISHINA EFFECTS IN GAMMA-RAY BURSTS

Synchrotron and/or SSC are most likely playing a major role in the emission from both long and short GRBs (for recent reviews, see Piran 2005; Meszaros 2006; Nakar 2007). GRB emission is composed of (at least) two physically distinctive phases—the prompt and afterglow emission. The prompt emission is observed as a short burst of ∼MeV gamma rays which lasts from a fraction of a second to several minutes. The radiation process that generates these photons is not determined yet (see recent discussion in Piran et al. 2009) although a fast cooling synchrotron emission is a popular model. The afterglow is observed for weeks and sometime even years in radio to X-ray wavelength. It is most likely that the radio to X-ray afterglow is a synchrotron emission (at first fast and later slow cooling) from a relativistic shockwave that propagates into the circum-burst medium.

6.1. Prompt Emission

We consider here cases in which prompt emission of GRBs is generated by fast cooling synchrotron emission. Since the observed spectra of GRBs peak around a fraction of MeV we have approximately $h\nu_m \sim m_e c^2$ implying that

$$\widehat{\gamma_m} \approx \Gamma. \tag{57}$$

Opacity constraints (e.g., Lithwick & Sari 2001) indicates that $\Gamma \gtrsim 100$, while considerations such as the afterglow onset suggest $\Gamma \lesssim 1000$. In the internal shock scenario the radiating electrons are accelerated by mildly relativistic shocks and therefore $\gamma_m \sim 100$. Thus, it is likely that in some, and maybe even in a significant fraction, of the GRBs $\widehat{\gamma_m}/\gamma_m \sim 1$ during the prompt emission and therefore, KN effects play an important role in shaping the observed prompt MeV spectrum. It is not clear however that the theory of optically thin SSC emission that is discussed in this paper is directly applicable to the prompt emission of all bursts. The reason is that here we assume that the synchrotron photons are optically thin for pair production of SSC photons. This assumption is justified if the prompt emission is produced at rather large radii ($\sim 10^{15}$–10^{16} cm), which is most likely in cases where the variability timescale is longer than a few seconds. It is violated however, in most cases, if the prompt emission is generated at smaller radii of $\sim 10^{13}$ cm.

We therefore expect that our results are applicable at least in some of the bursts. The expected observational KN signature may have already been observed. The prompt emission spectrum of GRBs is typically fitted by a broken power law with a F_ν low-energy spectral index α_L and high-energy spectral index α_H. For long GRBs, the value of α_L is between -1 and 1 while the value of α_H is between -0.5 and -2.5 (Preece et al. 2000; Kaneko et al. 2006). The standard synchrotron fast cooling model (that ignore KN effects) predicts $\alpha_L \approx -0.5$ and $\alpha_H = -p/2$ which is clearly inconsistent with many of the observed bursts (e.g., Preece et al. 1998; Kumar & McMahon 2008). Preece et al. (1998) point out that $\alpha_L > 1/3$ is inconsistent with optically thin synchrotron spectrum (the so-called 'line of death') while $-0.5 < \alpha_L$ is inconsistent with synchrotron emission from fast cooling electrons, which is required by the high efficiency of the prompt phase. When KN effects are considered α_L can be as high as 0 and α_H can be as high as $-(p-1)/2$. Thus, KN effects may be the reason for the hard spectrum observed in some of the prompt emission spectra also in cases that we observe synchrotron emission from fast cooling electrons, although it cannot explain cases where $\alpha_L < 0$.

6.2. Afterglow

Afterglow theories provide an approximate description of the observed afterglow multi-wavelength light curve for a given set

of physical conditions (e.g., blast wave energy, external density profile, initial jet structure, etc.). Incorporating the KN effects described in Sections 3 and 4 is straightforward. Here, we show the result of applying KN effects to the external-shock theory of a spherical blast wave that propagates into a constant external density (e.g., Sari et al. 1998). Within the framework of this theory

$$\nu_m = 5\cdot 10^{11}\epsilon_{e,-1}^{2}\epsilon_{B,-3}^{1/2}E_{53}^{1/2}T_{\rm day}^{-3/2}\,{\rm Hz},$$
$$\nu_c = 3\cdot 10^{16}\epsilon_{B,-3}^{-3/2}E_{53}^{-1/2}n^{-1}T_{\rm day}^{-1/2}[1+Y(\gamma_c)]^{-2}\,{\rm Hz}, \quad (58)$$

where E is the isotropic equivalent energy of the blast wave, n is the external medium density, and $T_{\rm day}$ is the observed time since the explosion in units of days (we neglect here redshift effects). Q_x denotes the value of the quantity Q in units of 10^x (c.g.s). Note the explicit dependence of the r.h.s of the equation for ν_c on γ_c. The magnetic field in the shocked fluid rest frame is $B\approx 0.1\epsilon_{B,-3}^{1/2}E_{53}^{1/8}n^{3/8}T_{\rm day}^{-3/8}$ G, implying that

$$\gamma_{\rm self}\approx 7.5\cdot 10^{5}\epsilon_{B,-3}^{1/6}E_{53}^{1/24}n^{1/8}T_{\rm day}^{-1/8} \quad (59)$$

depends very weakly on the physical parameters. Since electrons are expected to be accelerated to much higher values than $\gamma_{\rm self}$, KN effects may affect the observed afterglow.

Starting several minutes after the burst we expect the afterglow to be in its slow cooling phase. During this phase, we use Equations (4) and (47) to find $Y(\gamma_c)$ and $\widehat{\gamma_c}/\gamma_c$ in the various regimes

$$Y(\gamma_c)\approx\begin{cases} 5\,e^{\frac{4(2.4-p)}{4-p}}\,\epsilon_{e,-1}^{\frac{p-1}{4-p}}\,\epsilon_{B,-3}^{-\frac{3-p}{4-p}}\,E_{53}^{\frac{p-2}{2(4-p)}}\,n^{\frac{p-2}{2(4-p)}}\,T_{\rm day}^{-\frac{p-2}{2(4-p)}} \\ \quad \widehat{\gamma_c}\gg\gamma_c;\ Y(\gamma_c)\gg 1 \\ e^{\frac{27.5-9.7p}{p-1}}\,\epsilon_{e,-1}^{2}\,\epsilon_{B,-3}^{\frac{3-p}{2(p-1)}}\,E_{53}^{\frac{1}{p-1}}\,n^{\frac{5-p}{2(p-1)}}\,T_{\rm day}^{-\frac{p-2}{p-1}} \\ \quad \widehat{\gamma_c}\ll\gamma_c;\ Y(\gamma_c)\gg 1 \\ e^{15.4-5.4p}\,\epsilon_{e,-1}^{p-1}\,\epsilon_{B,-3}^{-(3-p)}\,E_{53}^{\frac{p-2}{2}}\,n^{\frac{p-2}{2}}\,T_{\rm day}^{-\frac{p-2}{2}} \\ \quad \widehat{\gamma_c}\gg\gamma_c;\ Y(\gamma_c)\ll 1 \\ e^{13.8-4.8p}\,\epsilon_{e,-1}^{p-1}\,\epsilon_{B,-3}^{\frac{3-p}{4}}\,E_{53}^{\frac{1}{2}}\,n^{\frac{5-p}{4}}\,T_{\rm day}^{-\frac{p-2}{2}} \\ \quad \widehat{\gamma_c}\ll\gamma_c;\ Y(\gamma_c)\ll 1 \end{cases} \quad (60)$$

and

$$\frac{\widehat{\gamma_c}}{\gamma_c}\approx\begin{cases} 35\,e^{\frac{11(2.4-p)}{4-p}}\,\epsilon_{e,-1}^{\frac{3(p-1)}{4-p}}\,\epsilon_{B,-3}^{\frac{p+2}{2(4-p)}}\,E_{53}^{\frac{p+2}{2(4-p)}}\,n^{\frac{3}{(4-p)}}\,T_{\rm day}^{-\frac{3(p-2)}{2(4-p)}} \\ \quad \widehat{\gamma_c}\gg\gamma_c;\ Y(\gamma_c)>1 \\ 0.35\,e^{\frac{83-29p}{p-1}}\,\epsilon_{e,-1}^{6}\,\epsilon_{B,-3}^{\frac{p+2}{p-1}}\,E_{53}^{\frac{p+2}{p-1}}\,n^{\frac{6}{p-1}}\,T_{\rm day}^{-\frac{3(p-2)}{p-1}} \\ \quad \widehat{\gamma_c}\ll\gamma_c;\ Y(\gamma_c)>1 \\ 0.35\,\epsilon_{B,-3}^{5/2}\,E_{53}\,n^{3/2} \\ \quad Y(\gamma_c)<1. \end{cases} \quad (61)$$

For typical sets of long GRB parameters ($\epsilon_e\sim 0.1$, $\epsilon_B\sim 10^{-3}$–10^{-2}, $p=2.1$–2.7, $E_{53}=0.1$–10, and $n=0.1$–$1{\rm cm}^{-3}$) we have $Y(\gamma_c)\sim$ 1–10 and $\widehat{\gamma_c}/\gamma_c\gtrsim 1$. This implies that the SSC energy output of bright long GRBs (assuming canonical physical parameters) is only weakly affected by the KN limit. The cooling frequency in this regime ($Y(\gamma_c)>1$ and $\widehat{\gamma_c}>\gamma_c$) is

$$\nu_c\approx 10^{15}\,e^{\frac{8(p-2.4)}{4-p}}\,\epsilon_{e,-1}^{-\frac{2(p-1)}{4-p}}\,\epsilon_{B,-3}^{-\frac{p}{2(4-p)}}\,E_{53}^{-\frac{p}{2(4-p)}}\,n^{-\frac{2}{4-p}}\,T_{\rm day}^{-\frac{(8-3p)}{2(4-p)}}\,{\rm Hz}, \quad (62)$$

which for $p\neq 2$ can be significantly different than the standard expression when SSC cooling is included and KN effects are neglected. For example, here ν_c is independent of T for $p=8/3$ where in the standard model $\nu_c\propto T^{-1/2}$ for any p value. The synchrotron spectrum is affected at

$$\widehat{\nu_c}\approx 10^{18}\,e^{\frac{15(2.4-p)}{4-p}}\,\epsilon_{e,-1}^{\frac{4(p-1)}{4-p}}\,\epsilon_{B,-3}^{\frac{4+p}{2(4-p)}}\,E_{53}^{\frac{4+p}{2(4-p)}}\,n^{\frac{4}{4-p}}\,T_{\rm day}^{-\frac{(3p-4)}{2(4-p)}}\,{\rm Hz}, \quad (63)$$

where the synchrotron spectral index becomes slightly harder ($-0.75(p-1)$ instead of $-p/2$). This KN signature of spectral hardening may be observed in the X-ray.

ϵ_B is one of the least constrained parameters in GRB external shocks and while $\epsilon_B=10^{-3}-10^{-2}$ seems to be a favorable value, ϵ_B may be significantly smaller. However, smaller ϵ_B does not necessarily imply larger value of $Y(\gamma_c)$, whereas, naively, the opposite is expected by a model that neglects KN effects where $Y(\gamma)=Y_{\rm noKN}=\sqrt{\epsilon_e/\epsilon_B}$. Equation (60) shows that for $\widehat{\gamma_c}>\gamma_c$ the value of $Y(\gamma_c)$ increases when ϵ_B is reduced (assuming $Y(\gamma_c)>1$). However, for $\widehat{\gamma_c}<\gamma_c$ the value of $Y(\gamma_c)$ decreases when ϵ_B is reduced. The reason is that in the latter regime the KN suppression becomes stronger when ϵ_B is reduced. As a result, if we allow ϵ_B to vary, while holding the rest of the parameters constant, $Y(\gamma_c)$ is maximized once $\widehat{\gamma_c}=\gamma_c$,

$$Y_{\rm max}(\gamma_c)\approx 10\,e^{\frac{27(3.2-p)^2-17}{(p+2)(4-p)}}\,\epsilon_{e,-1}^{\frac{5(p-1)}{p+2}}\,E_{53}^{1/2}\,n^{\frac{8-p}{2(p+2)}}\,T_{\rm day}^{-\frac{5(p-2)}{2(p+2)}}. \quad (64)$$

For the canonical values of the parameters taken here ($E_{53}=1$, $\epsilon_e=0.1$ and $n=1{\rm cm}^{-3}$) this maximum is achieved at $\epsilon_B\sim 10^{-4}$. Equation (64) implies that in bursts that are not very bright ($E<10^{51}$ erg and $n<1{\rm cm}^{-3}$) the SSC cooling is suppressed for any value of ϵ_B and the synchrotron emission is better approximated by ignoring SSC cooling than by including it but ignoring KN effects. It also implies that there is no significant SSC GeV emission accompanying late afterglows that are not very luminous in radio to X-ray emission. This includes most (and maybe all) of the short GRBs (see also discussion in Nakar 2007).

During the first several minutes the afterglow is often cooling fast, in which case the importance of the KN effects are determined by the ratio $\widehat{\gamma_m}/\gamma_m$,

$$\frac{\widehat{\gamma_m}}{\gamma_m}\approx 100\,\epsilon_{e,-1}^{-3}\,\epsilon_{B,-3}^{-1/2}\,E_{53}^{-1/2}\,T_2^{3/2}, \quad (65)$$

where $T_2=T/100$ s. This implies that according to the standard external shock model the energy output of the SSC emission during the early afterglow is not strongly affected by the KN limit.

7. SUMMARY

In this paper, we present analytic approximation to the optically thin synchrotron-SSC spectra in case that the distribution of the radiating electrons is modified by the KN cross-section. We consider here cases where there is only a single SSC scattering and multiple photon upscatterings are entirely suppressed by the KN cross section. We also consider only systems which are optically thin to pair production by the SSC photons. These analytic expressions are useful for construction of analytic and semianalytic theory of radiation from astrophysical sources, such as GRBs, AGNs, and pulsar wind nebula, where KN effects may be important.

We find six general spectral types (with some subcases within these six types) that differ mostly by the level of SSC suppression by the KN cross section. Table 1 summarizes the physical

conditions that result in each of the spectral types. It also points to the relevant section in the paper that discusses the case as well as the relevant equations of $Y(\gamma)$, $F_\nu^{\rm syn}$, and $F_\nu^{\rm IC}$.

The main effect of the KN limit on the electron distribution is the additional dependence of the cooling rate on the electron Lorentz factor. Electrons with higher Lorentz factor can upscatter a smaller fraction of the synchrotron photons and are therefore cooling more slowly compared to the case where the KN limit is ignored. The result is the introduction of new critical values of Lorentz factors which correspond to new synchrotron and SSC power-law segments. The new critical Lorentz factors differ between the spectral cases and are typically one or more of $\widehat{\nu_m}$, $\widehat{\nu_c}$, ν_0 and $\widehat{\nu_0}$, (γ_0 is defined so $Y(\gamma_0)=1$ and $\widehat{\gamma}$ is defined in Equation (4)). Table 2 summarizes the value of the critical Lorentz factors in each of the cases as a function of ϵ_e/ϵ_B, γ_m, γ_c, $\widehat{\gamma_m}$, and $\widehat{\gamma_c}$. The new power-law indices, and there frequency range, that are introduced to the synchrotron spectrum by the KN limit are summarized in Table 3. The ratio of inverse Compton to synchrotron cooling, i.e., $Y(\gamma)$, is always a decreasing function. Therefore, synchrotron power-law segments that are introduced by KN effects are always harder than, or comparable to, those that are predicted by standard synchrotron theories, which ignore the KN limit.

The hardening of the synchrotron spectrum results in two main observable features that should be taken into account when an observed synchrotron spectrum is analyzed. First, a spectrum of the fast cooling regime can asymptotically be as hard as $F_\nu \propto \nu^0$. Such a power-law segment is observed when the electrons which are radiating the synchrotron photons within this power-law segment are cooled down predominantly by upscattering synchrotron photons within this power-law segment itself (Cases IIb and IIc). This flat spectrum is significantly different than any of the predictions of a standard synchrotron theory that ignore KN effects, as standard theory predicts spectral indices that are harder than $1/3$ or softer than $-1/2$. Note that the actual spectrum in this specific segment is significantly smoother than the analytic approximation. As a result α in this power-law segment may approach the asymptotic value $\alpha = 0$ only for very large values of ϵ_e/ϵ_B. For example, numerical solution of Equations (9), (10), and (15) shows that if $\epsilon_e/\epsilon_B = 100$ the α value in this segment cannot exceed ≈ -0.3 while if $\epsilon_e/\epsilon_B = 10^4$ it cannot exceed ≈ -0.2. Second, $\nu_{\rm syn}^{\rm peak}$ is typically an available observable even when the spectral resolution is limited, and standard theory associates it with ν_m in the fast cooling regime and ν_c in the slow cooling regime. KN effects can modify this interpretation as the suppressed cooling of higher energy electrons may results in $\nu_{\rm syn}^{\rm peak} \approx \nu_0 > \max\{\nu_m, \nu_c\}$.

The SSC spectrum is also modified by KN limit. The most observable signature of KN effects in the SSC spectrum is the "KN cutoff," which is actually not a sharp cutoff but a consecutive set of power-law segments that become steeper at higher frequencies. The power-law segments and their physical origin are summarized in Table 4. In all cases, the SSC energy output is dominated by γ_m [γ_c] electrons in the fast [slow] cooling regime. Therefore emission at $\nu > \nu_{\rm peak}^{\rm IC}$ that is affected by the KN limit is dominated by electrons with $\gamma > \gamma_m [\gamma > \gamma_c]$ in the fast[slow] cooling regime. If these electrons are still cooling predominantly by SSC emission (i.e., their $\gamma < \gamma_0$) then the first KN break at $\nu > \nu_{\rm peak}^{\rm IC}$ is to a very mild spectral index, $-p+1$, and if $p \approx 2$ it is hardly distinguishable from the $-p/2$ spectral index expected in case that KN effects are unimportant. A clear steepening in the light curve can be observed only once the Lorentz factor of the upscattering electron is $\gamma > \widehat{\gamma_m}$ [$\gamma > \widehat{\gamma_c}$] in the fast [slow] cooling regime. At this point the SSC spectral index depends on the synchrotron spectral index of the upscttered photons (at $\widehat{\nu}$) and it ranges between $-p+1/2$ to $-p-1/3$. The value of $\nu_{\rm peak}^{\rm IC}$ is also affected by the KN cross section when $\widehat{\gamma_m} < \gamma_m$ [$\widehat{\gamma_c} < \gamma_c$] in the fast [slow] cooling regime. In these cases $\nu_{\rm peak}^{\rm IC} \approx 2\nu_m\gamma_m\widehat{\gamma_m}$ [$\nu_{\rm peak}^{\rm IC} \approx 2\nu_c\gamma_c\widehat{\gamma_c}$] instead of the standard value ($\approx 2\nu_m\gamma_m^2$ [$\approx 2\nu_c\gamma_c^2$]).

The KN cross-section can also affect the value of ν_c and in some cases can result in a unique temporal evolution—ν_c can "jump" by orders of magnitude over a short time scale. When KN effects are ignored the cooling rate of an electron always increases with its energy. The KN modified SSC cooling can revise this property introducing similar cooling rates for high-energy electrons that cool by synchrotron emission and much lower energy electrons that cool by SSC emission, where the cooling rate of intermediate energy electrons is much lower. When the similar cooling time of the high-energy electrons and low-energy electrons in such configuration becomes comparable to the system lifetime, t there is a sudden change of the observed ν_c between the frequency that corresponds to high-energy synchrotron cooling electrons ($\gamma_{c,\max,0}$) and the frequency that corresponds to low-energy SSC cooling electrons ($\gamma_{c,\min,0}$). This transition between $\gamma_{c,\max,0}$ and $\gamma_{c,\min,0}$ is completed over a short time scale (comparable to t). Table 2 summarizes the values of $\gamma_{c,\max,0}$ and $\gamma_{c,\min,0}$ for cases in which such sudden variation may be observed.

We demonstrate an application of our results to the a synchrotron model of the prompt emission of GRBs. We find that signature of KN effects may have already been observed in the prompt emission of some GRBs, in the form of spectrum that is harder than the standard synchrotron model both above and below $\nu_{\rm syn}^{\rm peak}$. We examine also the application of the KN limit to the external shock model (in its quasi-spherical regime) of GRB afterglow emission. Here we find that in the slow cooling phase, assuming canonical parameters: (1) $\widehat{\nu_c}$ may be observed passing through the X-ray, (2) the value of ν_c may be significantly modified by the KN limit, (3) the SSC GeV energy output is unlikely to be suppressed by the KN cross section when the radio -X-ray afterglow is luminous, but it may be strongly suppressed when the radio-X-ray afterglow is faint. Finally we find that this afterglow model does not predict a large SSC-to-synchrotron luminosity ratio even in case that the poorly constrained model parameter ϵ_B is very small. The reason is that a low value of ϵ_B results in a strong KN suppression of the SSC luminosity. This result implies that ϵ_B cannot be easily deduced even if the SSC to synchrotron luminosity ratio of slow cooling GRB afterglow is accurately measured.

We thank Tsvi Piran, Pawan Kumar, and Orly Gnat for helpful discussions. R.S. was partially supported by ERC, ATP, and IRG grants, and a Packard Fellowships. This research was partially supported by the Israel Science Foundation (Grant No. 174/08).

REFERENCES

Ando, S., Nakar, E., & Sari, R. 2008, ApJ, 689, 1150
Böttcher, M., & Dermer, C. D. 2002, ApJ, 564, 86
Coppi, P. S. 1992, MNRAS, 258, 657
Derishev, E. V., Kocharovsky, V. V., Kocharovsky, V. V., & Mészáros, P. 2003, in AIP Conf. Ser. 662, Gamma-Ray Burst and Afterglow Astronomy 2001: A Workshop Celebrating the First Year of the HETE Mission, ed. G. R. Ricker & R. K. Vanderspek (Melville, NY: AIP), 292

Dermer, C. D., Böttcher, M., & Chiang, J. 2000, ApJ, 537, 255
Fan, Y., & Piran, T. 2006, MNRAS, 370, L24
Fan, Y.-Z., Piran, T., Narayan, R., & Wei, D.-M. 2008, MNRAS, 384, 1483
Granot, J., Piran, T., & Sari, R. 2000, ApJ, 534, L163
Kaneko, Y., Preece, R. D., Briggs, M. S., Paciesas, W. S., Meegan, C. A., & Band, D. L. 2006, ApJS, 166, 298, arXiv:astro-ph/0601188
Kumar, P., & McMahon, E. 2008, MNRAS, 384, 33
Li, H., & Kusunose, M. 2000, ApJ, 536, 729
Lithwick, Y., & Sari, R. 2001, ApJ, 555, 540
Mastichiadis, A., & Kirk, J. G. 1997, A&A, 320, 19
Meszaros, P. 2006, Reports of Progress in Physics, 69, 2259
Meszaros, P., Rees, M. J., & Papathanassiou, H. 1994, ApJ, 432, 181
Nakar, E. 2007, Phys. Rep., 442, 166
Pe'er, A., & Waxman, E. 2005a, ApJ, 633, 1018
Pe'er, A., & Waxman, E. 2005b, ApJ, 628, 857
Petry, D., et al. 2000, ApJ, 536, 742
Piran, T. 2005, Rev. Mod. Phys., 76, 1143
Piran, T., Sari, R., & Zou, Y.-C. 2009, MNRAS, 393, 1107
Preece, R. D., Briggs, M. S., Mallozzi, R. S., Pendleton, G. N., Paciesas, W. S., & Band, D. L. 1998, ApJ, 506, L23
Preece, R. D., Briggs, M. S., Mallozzi, R. S., Pendleton, G. N., Paciesas, W. S., & Band, D. L. 2000, ApJS, 126, 19, arXiv:astro-ph/9908119
Rees, M. J. 1967, MNRAS, 137, 429
Sari, R., & Esin, A. A. 2001, ApJ, 548, 787
Sari, R., Piran, T., & Narayan, R. 1998, ApJ, 497, L17
Tavecchio, F., Maraschi, L., & Ghisellini, G. 1998, ApJ, 509, 608
Vurm, I., & Poutanen, J. 2009, ApJ, 698, 293
Zhang, B., et al. 2007, ApJ, 655, 989